

PHOTON COUNTING

Using Photomultiplier Tubes

INTRODUCTION

Recently, non-destructive and non-invasive measurement using light is becoming more and more popular in diverse fields including biological, chemical, medical, material analysis, industrial instruments and home appliances. Technologies for detecting low level light are receiving particular attention since they are effective in allowing high precision and high sensitivity measurements without changing the properties of the objects for low volume sample.

Biological and biochemical scrutinies use low-light-level measurement by detecting fluorescence emitted from cells labeled with a fluorescent dye. In clinical testing and medical diagnosis, various advanced techniques are being used, for example, invitro assay for blood analysis and blood cell counting, immunoassay for hormone testing and diagnosis of cancers and various infectious diseases, and diagnostic analysis of genes and single base polymorphism by using "gene chips". These techniques involve low-light-level measurement such as colorimetry, absorption spectroscopy, fluorescence photometry, and detection of light scattering or luminescence measurement. In molecular biology research, optical sensors occupy an important position as the fluorescence detectors in fluorescence correlation spectroscopy (FCS) - an innovative technique for analyzing dynamic interaction between molecules by detecting fluorescent molecules at single molecule levels. Furthermore, in RIA (radioimmunoassay) which has been used in immunological examinations using radioisotopes, radiation emitted from a sample is converted into low level light which must be measured with high sensitivity. In environmental measurement, test methods that make use of fluorescence and luminescence measurements are being used for hygiene monitoring such as for bacteria contamination in food processing and for water pollution. These test methods allow rapid measurement, yet with high sensitivity.

Photomultiplier tubes (PMT), photodiodes and CCD image sensors are widely used as "eyes" for detecting low level light. These detectors convert light into analog electrical signals (current or voltage) in most applications. However, when the light level becomes weak so that the incident photons are detected as separate pulses, the single photon counting method using a photomultiplier tube is very effective if the average time intervals between signal pulses are sufficiently wider than the time resolution of the photomultiplier tube. This photon counting method is superior to analog signal measurement in terms of stability, detection efficiency and signal-to-noise ratio.

This technical manual explains how to use photomultiplier tubes in photon counting to perform low-light-level measurement with high sensitivity and high accuracy. This manual also describes the principle of photon counting, its key points and operating circuit configuration, as well as characteristics of photomultiplier tubes and their selection guide.

TABLE OF CONTENTS

1. What is Photon Counting ?	2
1-1 Analog Mode and Digital Mode (Photon Counting Mode)	
1-2 The Principle of Photon Counting	
2. Operation and Characteristics of Photon Counting	5
2-1 Photon Counter and Multichannel Pulse Height Analyzer	
2-2 Basic Characteristics in Photon Counting	
(1) Pulse Height Distribution and Plateau Characteristics	
(2) Output Instability vs. Variations in Photomultiplier Tube Gain (current amplification)	
(3) Linearity of Count Rate	
3. Characteristics of Photomultiplier Tubes	9
3-1 Spectral Response (Quantum Efficiency)	
3-2 Collection Efficiency	
3-3 Supply Voltage and Gain	
3-4 Noise	
3-5 Magnetic Shield	
3-6 Stability and Dark Storage	
3-7 Uniformity	
3-8 Signal-to-Noise Ratio	
4. Measurement Systems	16
4-1 Synchronous Photon Counting Using Chopper	
4-2 Time-Resolved Photon Counting by Repetitive Sampling	
4-3 Time-Resolved Photon Counting by Multiple Gates	
4-4 Time-Correlated Photon Counting	
4-5 Calculating the Autocorrelation Function using a Digital Correlator	
5. Selection Guide	19
5-1 Selecting the Photomultiplier Tube	
5-2 Photomultiplier Tubes for Photon Counting	
5-3 Peripheral Devices	

1. What is Photon Counting ?

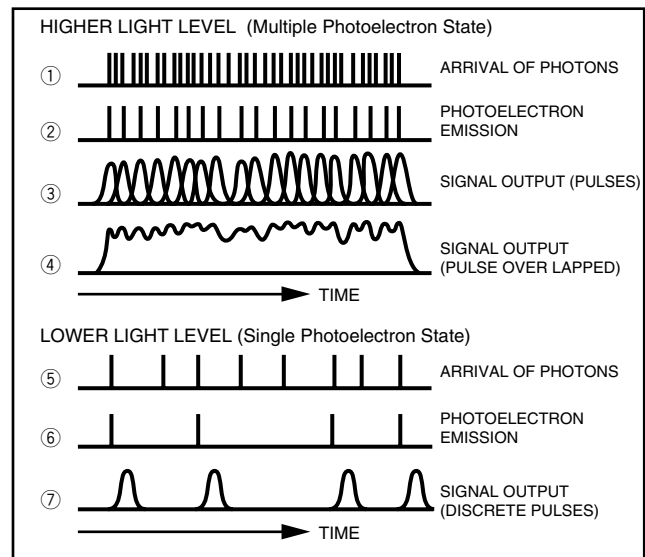
1-1 Analog Mode and Digital Mode (Photon Counting Mode)

A photomultiplier tube (PMT) consists of a photocathode, an electron multiplier (composed of several dynodes) and an anode. (See Figure 2 for schematic construction.) When light enters the photocathode of a photomultiplier tube, photoelectrons are emitted from the photocathode. These photoelectrons are multiplied by secondary electron emission through the dynodes and then collected by the anode as output pulses. In usual applications, these output pulses are not handled as individual pulses but dealt with as an analog current created by a multitude of pulses (so-called analog mode). In this case, a number of photons are incident on the photomultiplier tube per unit time as in ① of Figure 1 and the resulting photoelectrons are emitted from the photocathode as in ②. The photoelectrons multiplied by the dynodes are then derived from the anode as output pulses as in ③. At this point, when the pulse-to-pulse interval is narrower than each pulse width or the signal processing circuit is not fast enough, the actual output pulses overlap each other and eventually can be regarded as electric current with shot noise fluctuations as shown in ④.

In contrast, when the light intensity becomes so low that the incident photons are separated as shown in ⑤, the output pulses obtained from the anode are also discrete as shown in ⑦. This condition is called a single photoelectron state. The number of output pulses is in direct proportion to the amount of incident light and this pulse counting method has advantages in signal-to-noise ratio and stability over the analog mode in which an average of all the pulses is made.

This pulse counting technique is known as the photon counting method. Since the detected pulses undergo binary processing for digital counting, the photon counting method is also referred to as the digital mode.

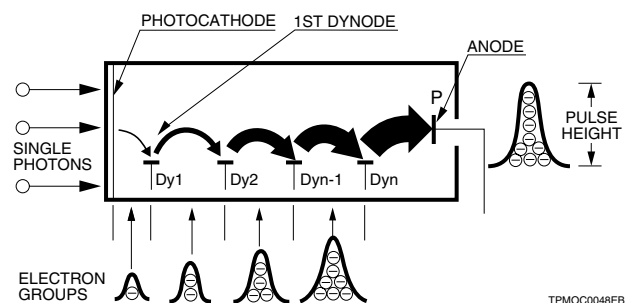
Figure 1 : Output Pulses from Photomultiplier Tube at Different Light Levels



1-2 The Principle of Photon Counting

One important factor in photon counting is the quantum efficiency (QE). It is the production probability of photoelectrons being emitted when one photon strikes the photocathode. In the single photoelectron state, the number of emitted photoelectrons (primary electrons) per photon is only 1 or 0. Therefore QE refers to the ratio of the average number of emitted electrons from the photocathode per unit time to the average number of photons incident on the photocathode.

Figure 2 : Photomultiplier Tube Operation in Single Photoelectron State



Photoelectrons emitted from the photocathode are accelerated and focused onto the first dynode (Dy1) to produce secondary electrons. However, some of these electrons do not strike the Dy1 or deviate from their normal trajectories, so they are not multiplied properly. This efficiency of collecting photoelectrons is referred to as the collection efficiency (CE). In addition, the ratio of the count value (the number of output pulses) to the number of incident photons is called the detection efficiency or counting efficiency, and is expressed by the following equation :

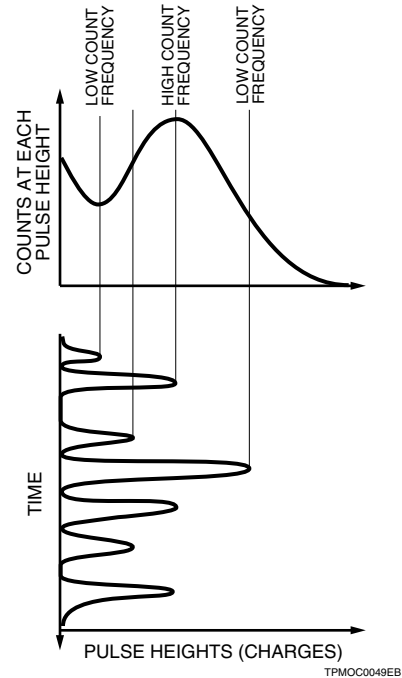
$$\begin{aligned} \text{Detection efficiency} &= N_d / N_p \\ &= \eta \cdot \alpha \end{aligned}$$

where N_d is the count value, N_p is the number of incident photons, η is the photocathode QE and α is the CE. Although it will be discussed later, detection efficiency also depends on the threshold level that brings the output pulses into a binary signal. Since the number of secondary electrons emitted from the Dy1 varies from several to about 20 in response to one primary electron from the photocathode, they can be treated by Poisson distribution in general, and the average number of secondary electrons becomes the secondary electron emission ratio δ . This holds true for multiplication processes in the subsequent dynodes. Accordingly, for a photomultiplier tube having n stages of dynodes, a single photoelectron from the photocathode is multiplied by δ^n to create a group of electrons and is derived from the anode as an output pulse. In this process, the height of each output pulse obtained at the anode depends on fluctuations in the secondary electron multiplication ratio stated above, so that it differs from pulse to pulse. (Figure 3)

Other reasons why the output pulse height becomes unequal are that gain varies with the position on each dynode and some deviated electrons do not contribute to the normal multiplication process. Figure 3 shows a histogram of the anode pulse heights. This graph is known as the pulse height distribution (PHD).

As illustrated in Figure 3, the photomultiplier tube output exhibits fluctuations in the pulse height and the PHD is obtained by time-integrating these output pulses at different pulse heights. The abscissa of this graph indicates the pulse height that represents the charge (number of electrons contained in one electron group) or the pulse voltage (current) produced by that electron group. It is generally expressed in the number of channels used for the abscissa of a multichannel analyzer.

Figure 3 : Photomultiplier Tube Output and PHD



Photomultiplier Tube Output in Single Photoelectron State

The output signal from a photomultiplier tube in the photon counting mode can be calculated as follows:

In the photon counting mode, a single photoelectron e^- (electron charge: $1.6 \times 10^{-19} \text{ C}$) is emitted from the photocathode. If the photomultiplier tube gain μ is 5×10^6 , then the anode output charge is given by

$$\begin{aligned} e \times \mu &= 1.6 \times 10^{-19} \cdot 5 \times 10^6 \text{ C} \\ &= 8 \times 10^{-13} \text{ C} \end{aligned}$$

Here, if the pulse width t (FWHM) of the anode output signal is 10 ns, then the output pulse peak current I_p is

$$\begin{aligned} I_p &= e \cdot \mu \cdot 1/t \text{ A} \\ &= (8 \times 10^{-13} \text{ C}) / (10 \times 10^{-9} \text{ s}) \\ &= 80 \mu \text{ A} \end{aligned}$$

This means that the anode output pulse width is narrower, we can obtain much higher output peak current. If the load resistance or input impedance of the succeeding amplifier is 50Ω , the output pulse peak voltage V_o becomes

$$\begin{aligned} V_o &= I_p \times 50 \Omega \\ &= 4 \text{ mV} \end{aligned}$$

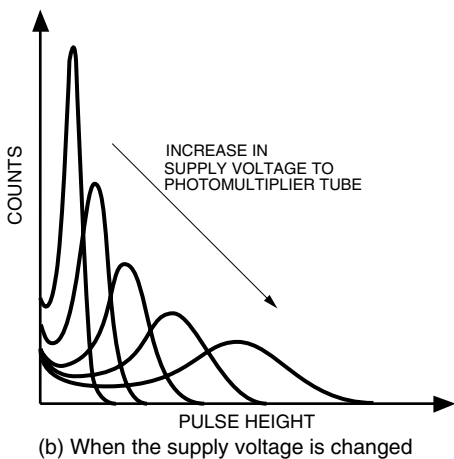
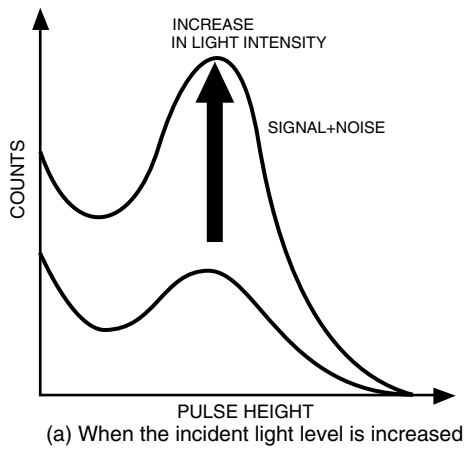
The amplitude of the photomultiplier tube output pulse in the photon counting mode is extremely small. This requires a photomultiplier tube having a high gain and may require an amplifier with sufficiently low noise relative to the photomultiplier tube output noise. As a general guide, photomultiplier tubes should have a gain of approximately 1×10^6 or more.

Figure 4 (a) shows a PHD when the incident light level is increased under single photoelectron conditions, and (b) shows a PHD when the supply voltage is changed.

The ordinate is the frequency of the output pulses that produce a certain height within a given time. Therefore, the distribution varies with the measurement time or the number of incident photons in the upper direction of the ordinate as shown in Figure 4 (a).

As explained above, the abscissa of the PHD represents the pulse height and is proportional to the gain of the photomultiplier tube and becomes a function of the supply voltage of the photomultiplier tube. This means that as the supply voltage changes, the PHD also shifts along the ordinate, but the total number of counts is almost constant.

Figure 4 : PHD Characteristics



TPHO0032EB

2. Operation and Characteristics of Photon Counting

This section describes circuit configurations for use in photon counting and the basic characteristics of photon counting measurements.

2-1 Photon Counter and Multichannel Pulse Height Analyzer

There are two methods of signal processing in photon counting: one uses a photon counter and the other a multichannel pulse height analyzer (MCA). Figure 5 shows the circuit configuration of each method and the pulse shapes obtained from each circuit system.

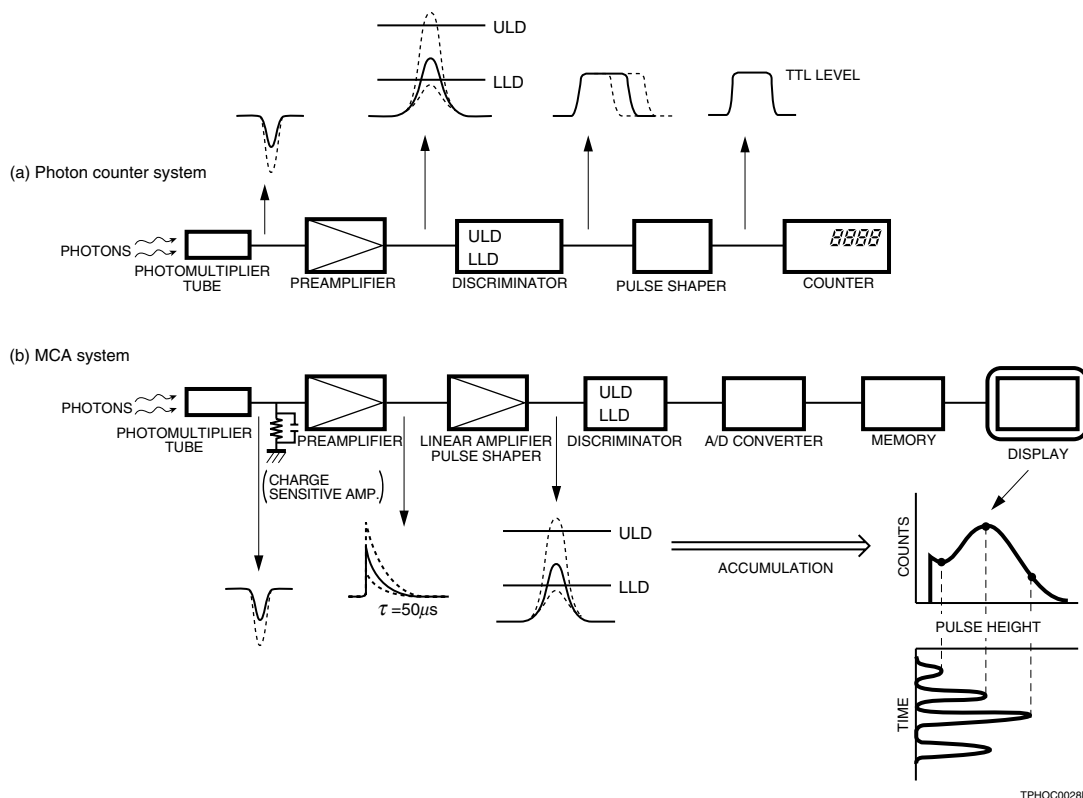
In the photon counter system of Figure 5 (a), the output pulses from the photomultiplier tube are amplified by the preamplifier. These amplified pulses are then directed into the discriminator. The discriminator compares the input pulses with the preset reference voltage to divide them into two groups: one group is lower and the other is higher than the reference voltage. The lower pulses are eliminated by the lower level discriminator (LLD) and in some

cases, the higher pulses are eliminated by the upper level discriminator (ULD). The output of the comparator takes place at a constant level (usually a TTL logic level or CMOS level). The pulse shaper forms rectangular pulses allowing counters to count the discriminated pulses.

In contrast, in the MCA system shown in Figure 5 (b), the output pulses from the photomultiplier tube are generally integrated through a charge-sensitive amplifier, amplified and shaped with the linear amplifier. These pulses are discriminated according to their heights by the discriminator and are then converted from analog to digital. They are finally accumulated in the memory and displayed on the screen. This system is able to output pulse height information and frequency (the number of counts) simultaneously, as shown in the figure.

The photon counter system is used to measure the number of output pulses from the photomultiplier tube corresponding to incident photons, while the MCA system is used to measure the height of each output pulse and the number of output pulses simultaneously. The former system is superior in counting speed and therefore used for general-purpose applications. The MCA system has the disadvantage in not being able to measure high counts, it is used for applications where pulse height analysis is required.

Figure 5 : Typical Photon Counting Systems



TPHOC0028EB

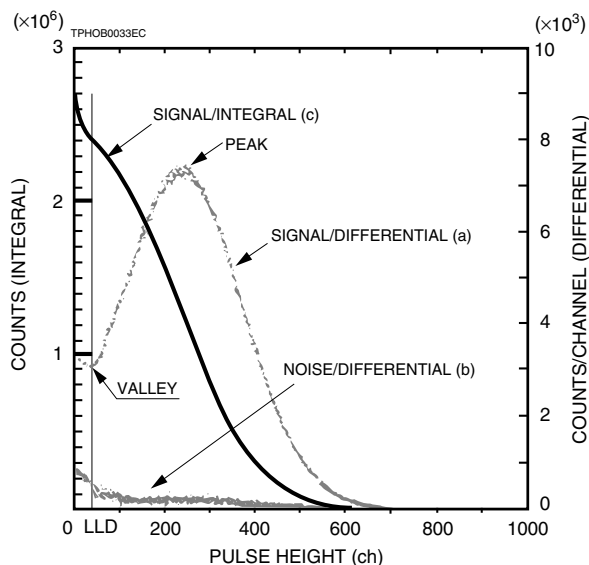
2-2 Basic Characteristics in Photon Counting

(1) Pulse Height Distribution and Plateau Characteristics

Figure 6 shows pulse height distributions (PHD) of a photomultiplier tube, obtained with an MCA. The curve (a) is the output when signal light is incident on the photomultiplier tube, while the curve (b) represents the noise when signal light is removed. The major noise component results from thermionic emission from the photocathode and dynodes. The PHD of such noise usually appears on the lower pulse height side. These PHD are the so-called differential curves and the lower level discrimination (LLD) is usually set at the valley of the curve (a). To increase detection efficiency, it is advantageous to set the LLD at a lower position, but this is also accompanied by a noise increase.

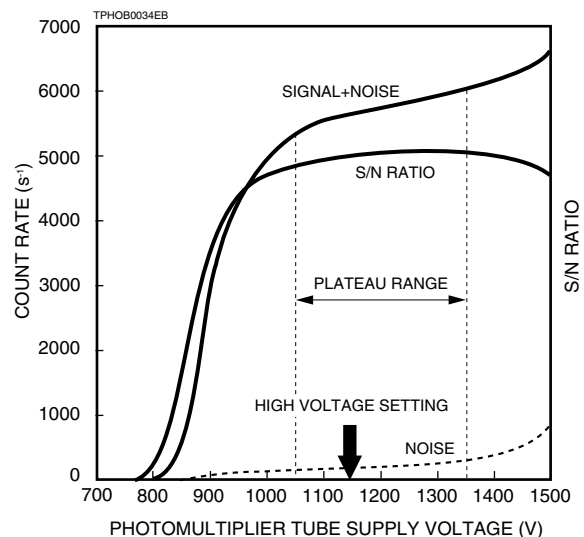
In contrast to the curve (a) in Figure 6, the curve (c) shows an integration curve in which the total number of pulses higher than a certain discrimination level have been plotted while changing the discrimination level. Since this integration curve (c) has an interrelation with the differential curve (a), the proper discrimination levels can be set in the photon counter system without using an MCA, by obtaining the integration curve instead.

Figure 6 : Differential and Integral Displays of PHD



The LLD stated above corresponds to a pulse height on a gentle slope portion in the integration curve. But this is not so distinct from other portions, making it difficult to determine the LLD. Another method using plateau characteristics is more commonly used. By counting the number of pulses with the LLD fixed while varying the supply voltage to the photomultiplier tube, a curve similar to the "SIGNAL+NOISE" curve shown in Figure 7 can be plotted. Although, analog gain increases exponentially with supply voltage, since the photomultiplier tube counts only the number of pulses, the slope of the curves is relatively flat, which makes the supply voltage setting easier. These curves are known as the plateau characteristics. The supply voltage for the photomultiplier tube should be set within this plateau region. It is also clear that plotting the signal-to-noise ratio shows a plateau range in the same supply voltage range. (See Section 3-8 (2).)

Figure 7 : Plateau Characteristics



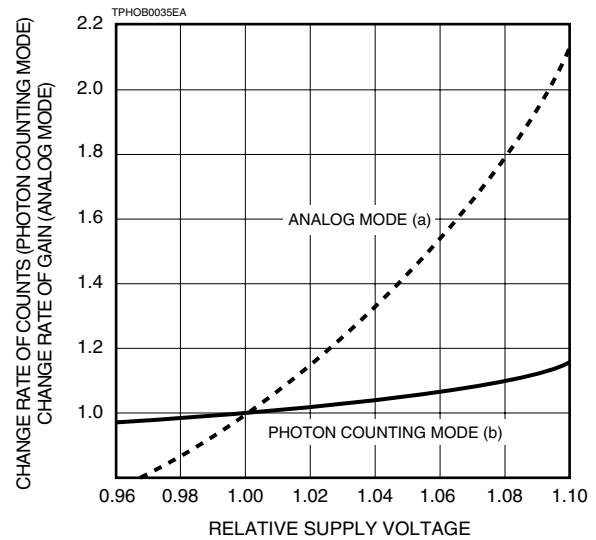
(2) Output Instability vs. Variations in Photomultiplier Tube Gain

If the photomultiplier tube gain varies for some reason (for example, a change in supply voltage or fluctuations in the ambient temperature, etc.), the output current of the photomultiplier tube is also affected and exhibits variations. In the analog mode the output current (or gain) of the photomultiplier tube changes with variations in the supply voltage as shown in Figure 8 (a). In the photon counting mode, the output count changes, but this is significantly smaller than in the analog mode.

By setting the supply voltage in the plateau region as shown in Figure 7, the photon counting mode can minimize changes in the count rate with respect to variations in the supply voltage without sacrificing the signal-to-noise ratio. This means that the photon counting mode ensures high stability even when the gain of the photomultiplier tube varies as the gain is a function of the supply voltage. For the above reasons, the photon counting mode offers

several times higher stability than the analog mode against variations in the operating conditions.

Figure 8 : Output Variation vs. Supply Voltage



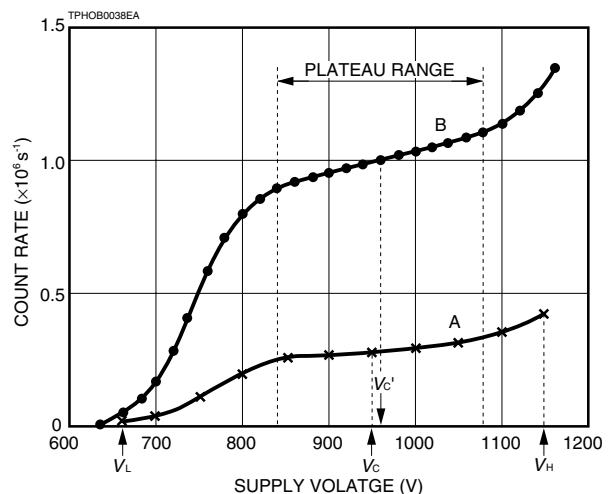
How to Obtain the Plateau

Speaking it in a broad sense, the integration curve explained in Section 2-2 (1) has plateau characteristics. Here we describe a more practical method for obtaining the plateau characteristics by varying the photomultiplier tube supply voltage.

1. Set up the photomultiplier tube, photon counter, high-voltage power supply, dark box, light source, etc, required to perform photon counting. Preferably, the photomultiplier tube should be stored in the dark box for about one hour after the setup has been completed.
2. Set the discrimination level (LLD) according to the instruction manual for the photon counter being used. Then allow a very small amount of light to strike the photomultiplier tube.
3. Gradually increase the photomultiplier tube supply voltage starting from about 500 V. When the photon counter begins to count any signal, halt there and make a plot of the supply voltage (V_L) and the counted value at that point, on a graph with the abscissa showing the supply voltage and the ordinate representing the count rate.
4. Increase the supply voltage with a 50 V step until it reaches about 90 % (V_H) of the maximum supply voltage while making plots on the graph. This will create a curve like "A" shown in Figure 9.

5. With the photomultiplier tube operated at a voltage (V_C) in the middle of the flat portion of curve "A", adjust the light source intensity so that the counted value is set to 10 % to 30 % of the maximum count rate of the photon counter.
6. Readjust the photomultiplier tube supply voltage to set at V_L , then make fine plots while changing the photomultiplier tube supply voltage in 10 V or 20 V steps. This will make a curve like "B" shown in Figure 9.
7. In the flat range (plateau range) on curve "B", the voltage V_C' at a point where the differential coefficient is smallest (minimum slope) will be the optimum PMT operating voltage.

Figure 9 : Plotting Plateau characteristics



(3) Linearity of Count Rate

The photon counting mode is generally used in very low-light-level regions where the count rate is low, and exhibits good linearity. However, when the amount of incident light becomes large, it is necessary to take the linearity of the count rate into account. The upper limit of the bandwidth of photomultiplier tubes ranges from 30 MHz to 300 MHz for periodical signal. However, the maximum count rate in the photon counting mode where random photos enter the photomultiplier tube is determined by the time response of photomultiplier tube and the time resolution of the signal processing circuit connected to the photomultiplier tube. The time resolution referred to here is defined as the minimum time interval between successive pulses that can be counted as separate pulses.

Figure 10 shows a typical linearity of the count rate obtained from a Hamamatsu H7360 Photon Counting Head. As can be seen from the figure, the dynamic range reaches as high as 10^7 s^{-1} . In this case, the linearity of the count rate is limited by the time resolution (pulse pair resolution) of the built-in circuit (18 ns).

If we let the measured count rate be $M \text{ (s}^{-1}\text{)}$ and the time resolution be $t \text{ (s)}$, the real count rate $N \text{ (s}^{-1}\text{)}$ can be approximated as follows:

$$N = \frac{M}{1 - Mt}$$

Figure 11 shows the actual data measured with the H7360 Photon Counting Head, along with the corrected data obtained with the above equation. This proves that after making correction, the photon counting mode provides an excellent linearity with a counting error of less than 1 %, even at a high count rate of 10^7 s^{-1} .

However, the linearity deviates from this corrected data curve in a region where measurement errors become large due to base line shift or overlapping of photomultiplier tube output pulses themselves.

Figure 10 : Linearity of Count Rate

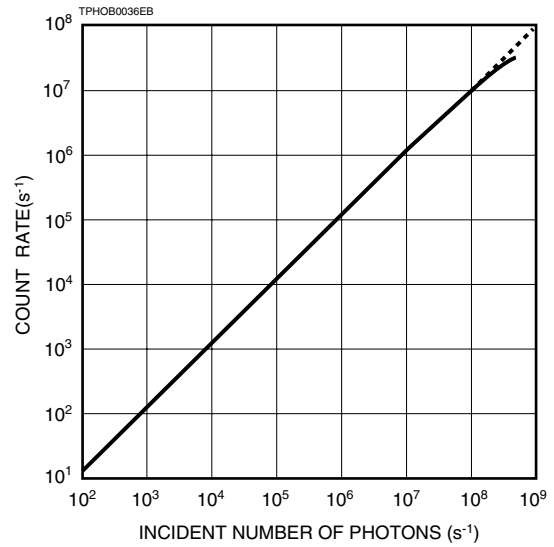
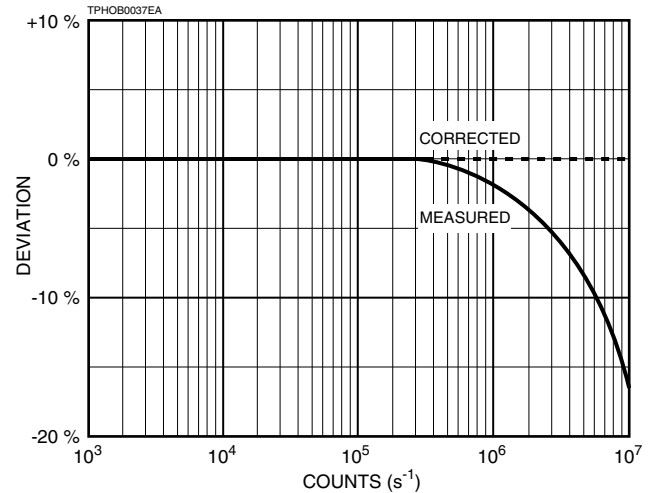


Figure 11 : Correction of Count Rate Linearity



3. Characteristics of Photomultiplier Tubes

3-1 Spectral Response (Quantum Efficiency)

When N number of photons enter the photocathode of a photomultiplier tube, the $N \times$ quantum efficiency (QE) of photoelectrons on average are emitted from the photocathode. The QE depends on the incident light wavelength and so exhibits spectral response.

Figures 12 (a) and (b) show typical spectral response characteristics for various photocathodes and window materials. The spectral response at wavelengths shorter than 350 nm is determined by the window material used, as shown in Figure 13.

In general, spectral response characteristics are expressed in terms of cathode radiant sensitivity or QE. The QE and

Figure 12 : Typical Spectral Response Characteristics

Figure 12(a): Transmission Mode Photocathodes

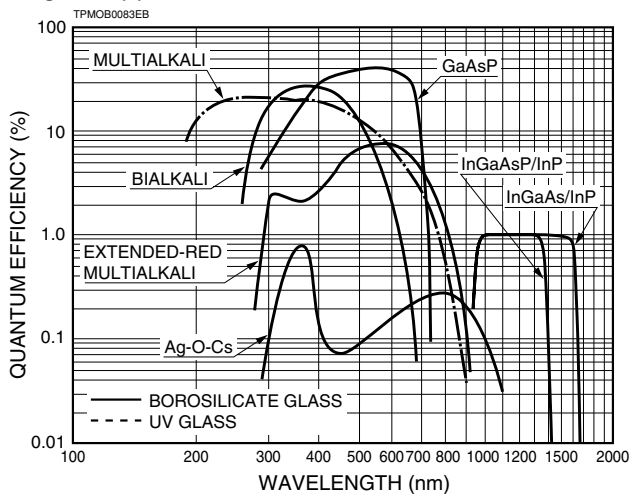
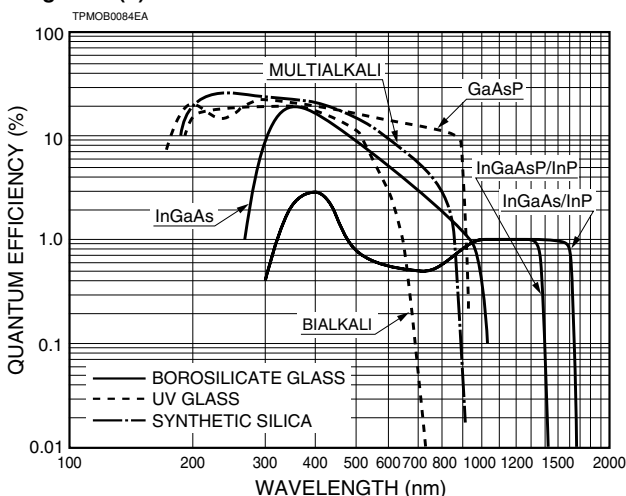


Figure 12(b): Reflection Mode Photocathodes

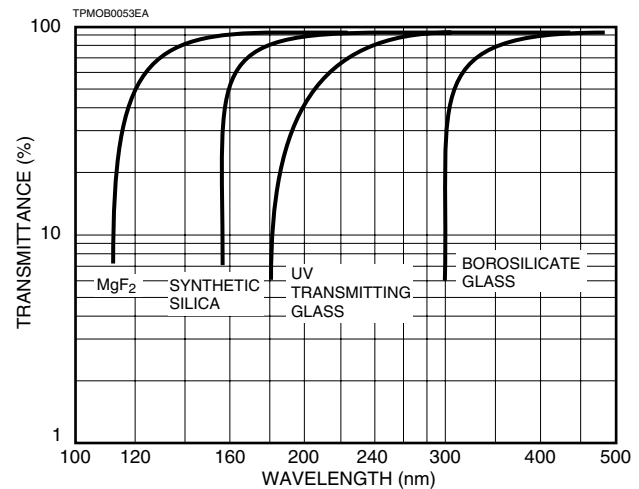


radiant sensitivity have the following relation at a given wavelength.

$$QE = \frac{S \times 1240}{\lambda}$$

where S is the cathode radiant sensitivity in amperes per watt (A/W) at the given wavelength λ in nanometers.

Figure 13 : Typical Transmittance of Window Materials



3-2 Collection Efficiency

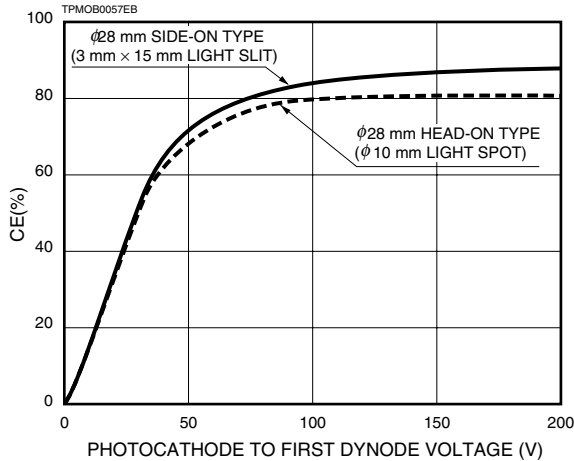
The collection efficiency (CE) is the probability in percent, that single photoelectrons emitted from the photocathode can be finally collected at the anode as the output pulses through the multiplication process in the dynodes. In particular, the CE is greatly affected by the probability that the photoelectrons from the photocathode can enter the first dynode and multiplied. Generally, the CE is from 70 % to 90 % for head-on photomultiplier tubes and 50 % to 70 % for side-on photomultiplier tubes with full cathode illumination.

The CE is very important in photon counting measurement. The higher the value of the CE, the smaller the signal loss, thus resulting in more efficient and accurate measurements. The CE is determined by the photocathode shape, dynode structure and voltage distribution for each dynode.

As stated earlier, the ratio of the number of signal pulses obtained at the anode to the number of photons incident on the photocathode is referred to as the detection efficiency or counting efficiency.

Figure 14 shows the relation between the CE and the photocathode to first dynode voltage of 28 mm (1-1/8 ") diameter photomultiplier tubes, measured in the photon counting mode with the discrimination level kept constant and with small area illumination. As can be seen, the CE sharply varies at voltages lower than 100 V, but becomes saturated and shows little change when the voltage exceeds this. This means that a sufficient voltage should be applied across the photocathode and the first dynode to obtain stable CE.

Figure 14 : CE vs. Photocathode to First Dynode Voltage



3-3 Supply Voltage and Gain

The output pulse height of a photomultiplier tube varies with the supply voltage change, even when the light level is kept constant. This means that the gain of the photomultiplier tube is a function of the supply voltage. The secondary emission ratio δ is the function of voltage E between dynodes and is given by

$$\delta = A \cdot E^\alpha$$

where A is the constant and α is determined by the structure and material of the electrodes, which usually takes a value of 0.7 to 0.8.

Here, if we let n denote the number of dynodes and assume that the δ of each dynode is constant, then the change in the gain μ relative to the supply voltage V is expressed as follows:

$$\begin{aligned} \mu &= \delta^n = (A \cdot E^\alpha)^n = \left\{ A \cdot \left(\frac{V}{n+1} \right)^\alpha \right\}^n \\ &= \frac{A^n}{(n+1)^{\alpha n}} \cdot V^{\alpha n} = K \cdot V^{\alpha n} \end{aligned}$$

(K is a constant.)

Since typical photomultiplier tubes have 9 to 12 dynode stages, the output pulse height is proportional to the 6th to 10th power of the supply voltage. The curve previously shown in Figure 8 for the analog mode represents this characteristic.

Figure 15 : Gain vs. Supply Voltage

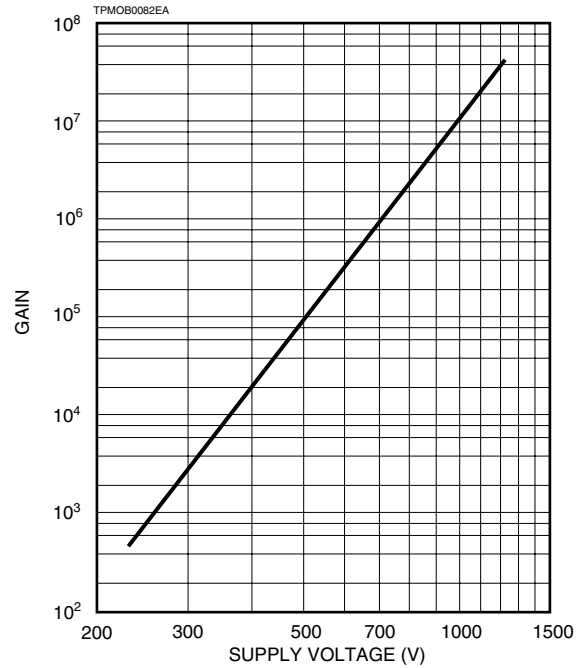
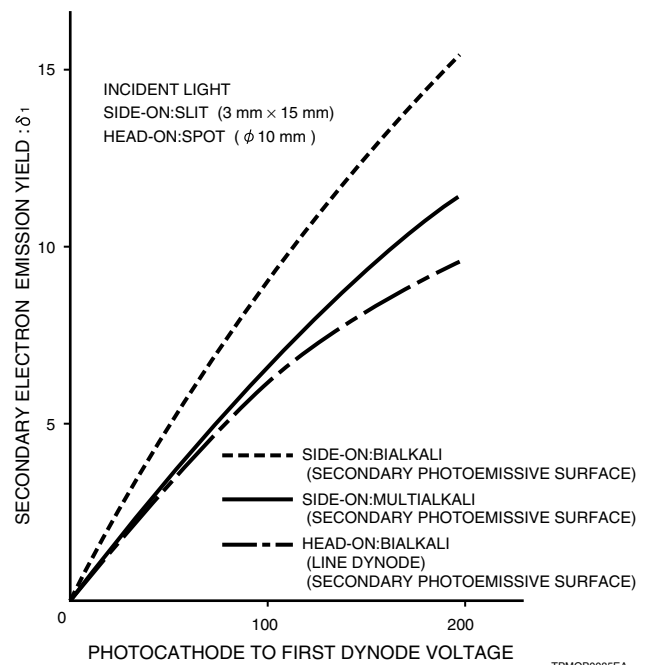


Figure 16 shows the relation between the secondary electron emission ratio (δ) and the photocathode to first dynode voltage. The incident light is passed through a slit of 3 mm x 15 mm for side-on photomultiplier tubes, or is focused on a spot of 10 mm diameter for head-on photomultiplier tubes. It is clear that the secondary electron emission ratio depends on the material of the secondary electron emission surface. Generally, the larger the secondary electron emission ratio, the better the PHD will be.

Figure 16 : Secondary Electron Emission Yield vs. Supply Voltage



3-4 Noise

Some noise exists in a photomultiplier tube even when it is kept in complete darkness. The noise adversely affect the counting accuracy, especially in cases where the count rate is low. The following precautions must be taken to minimize the noise effects.

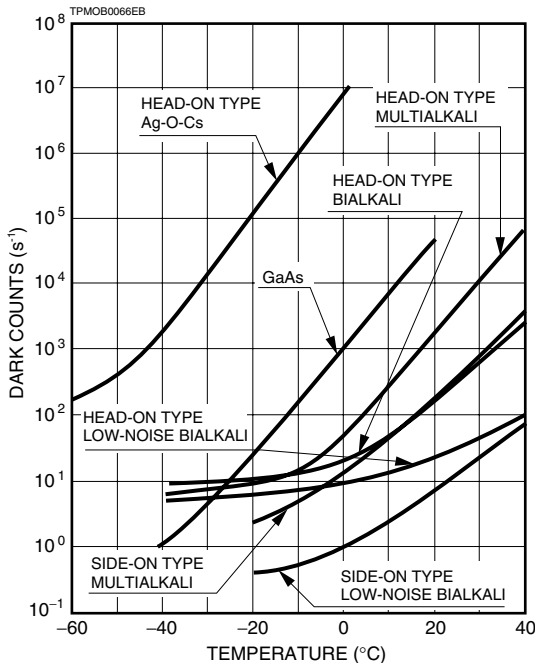
(1) Thermionic Emission of Electrons

Materials used for photocathodes and dynodes have low work functions (energy required to release electrons into vacuum), so they emit thermal electrons even at room temperatures. Most of the noise is caused by these thermal electrons mainly being emitted from the photocathode and amplified by the dynodes. Therefore, cooling the photocathode is the most effective technique for reducing noise in applications where low noise is essential. In addition, since thermal electrons increase in proportion to photocathode size, it is important to select the photocathode size as needed.

Figure 17 shows temperature characteristics of dark counts measured with various types of photocathodes. These are typical examples that vary considerably with photocathode type and sensitivity (especially red sensitivity).

The head-on type Ag-O-Cs, multialkali, and GaAs photocathodes have high sensitivity in the near infrared, but these photocathodes tend to emit large amounts of thermal electrons even at room temperatures, so usually cooling is necessary.

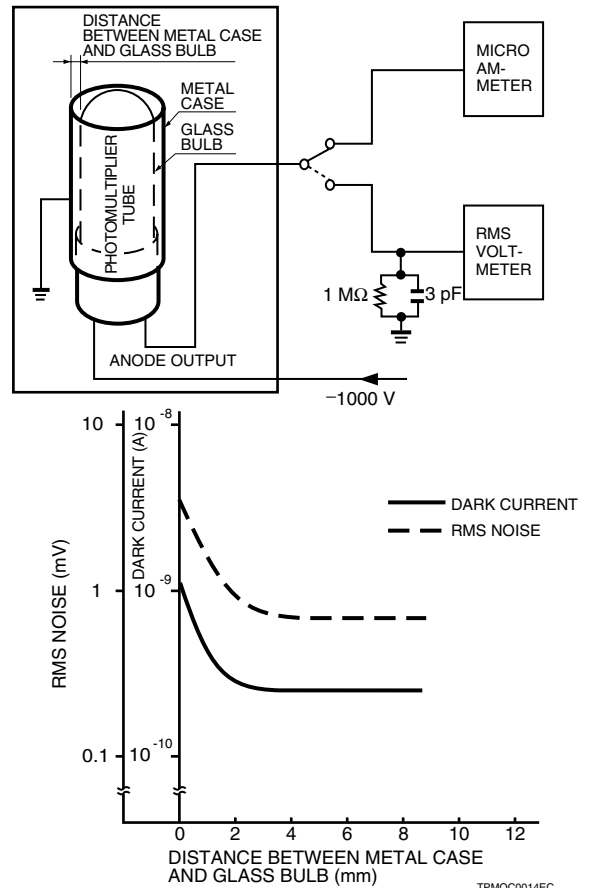
Figure 17 : Temperature Characteristics of Dark Counts



(2) Glass Scintillation

When electrons deviating from their normal trajectories strike the glass bulb of a photomultiplier tube, glass scintillation may occur and result in noise. Figure 18 shows typical dark current (RMS noise) versus the distance between the photomultiplier tube and the metal housing case at ground potential. This implies that glass scintillation noise is caused by stray electrons which are attracted to the glass bulb at a higher potential. This is particularly true when the tube is operated with a voltage divider circuit with the anode grounded. To minimize this problem, it is necessary to reduce the supply voltage for the photomultiplier tube, use a voltage divider circuit with the cathode grounded or make longer the distance between the photomultiplier tube and the housing. Another effective measure is to coat the outer surface of the glass bulb with conductive paint which is maintained at the photocathode potential in order to prevent stray electrons from being attracted to the glass bulb. In this case, however, the photomultiplier tube must be covered with an insulating material since a high voltage is applied to the glass bulb. We call this technique "HA coating". Although Figure 18 is an example of a side-on photomultiplier tube, similar characteristics will be observed for a head-on photomultiplier tube.

Figure 18 : Dark Current vs. Distance Between Photomultiplier Tube and Housing Case at Ground Potential



However, in most cases, the input window of the photomultiplier tube is exposed even with the HA coating. Therefore, in the anode grounded scheme, use of good insulating material such as fluorocarbon polymers or polycarbonate is necessary around the input window in negative HV operation. Otherwise, a large potential difference may be created at the input window, and could result in irregular and high dark counts.

To avoid this problem, adopting a cathode grounded scheme is strongly recommended.

(3) Leakage Current

Leakage current may be another source of noise. It may increase due to imperfect insulation of photomultiplier tube base or socket pins, and also due to contamination on the circuit board. It is therefore necessary to clean these parts with appropriate solvent like ethyl alcohol.

In addition, when a photomultiplier tube is used with a cooler and if high humidity is present, the photomultiplier tube leads and socket are subject to frost or condensation. This also results in leakage current and therefore special attention should be paid.

(4) Field Emission Noise

This is voltage-dependent noise. When a photomultiplier tube is operated at a high voltage near the maximum rating, a strong local electric field may induce a small amount of discharge causing dark pulses. It is therefore recommended that the photomultiplier tube be operated at a voltage sufficiently lower than the maximum rating.

(5) External Noise

Besides the noise from the photomultiplier tube itself, there are external noises that affect photomultiplier tube operation such as inductive noise. Use of an electromagnetic shield case is advisable. Vibration may also result in noise mixing into the signal.

(6) Ringing

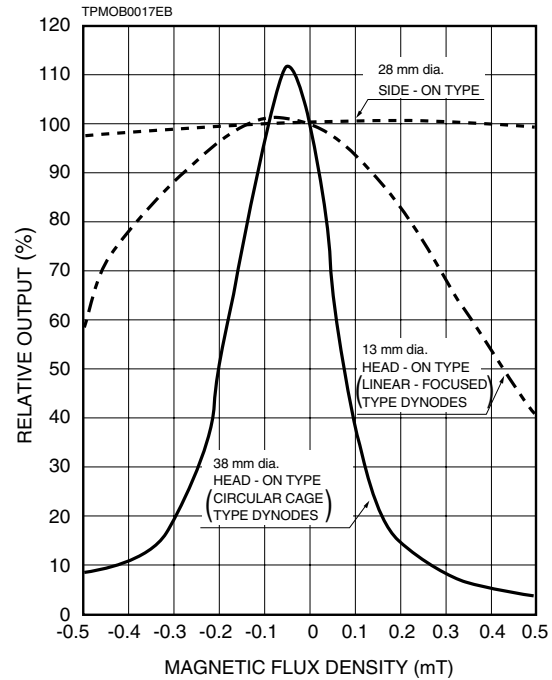
If impedance mismatching occurs in the signal output line from a photomultiplier tube, ringing may result, causing count error. This problem becomes greater in circuits handling higher speeds. The photomultiplier tube and the preamplifier should be connected in as short a distance as possible, and proper impedance matching should be provided at the input of the preamplifier.

3-5 Magnetic Shield

Most photomultiplier tubes are very sensitive to magnetic fields and the output varies significantly even with terrestrial magnetism (approx. 0.04 mT). Figure 19 shows typical examples of how photomultiplier tubes are affected by the presence of a magnetic field. Although photomultiplier

tubes in the photon counting mode are less sensitive to the magnetic field than in the analog mode, photomultiplier tubes should not be operated near any device producing a magnetic field (motor, metallic tools which are magnetized, etc.). When a photomultiplier tube has to be operated in a magnetic field, it is necessary to cover the photomultiplier tube with a magnetic shield case.

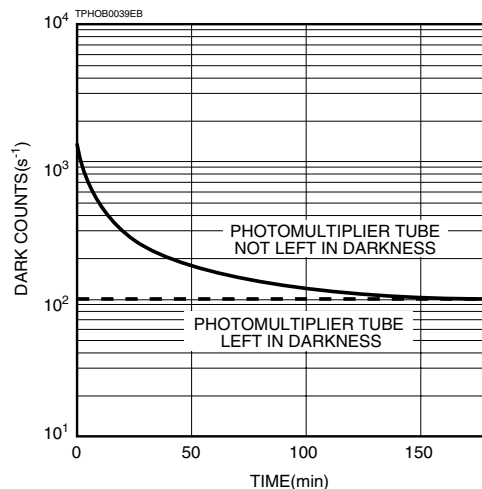
Figure 19 : Typical Effects by Magnetic Fields Perpendicular to Tube Axis



3-6 Stability and Dark Storage

In either the photon counting mode or analog mode, the dark current and dark count of a photomultiplier tube usually increase just after strong light is irradiated on the photocathode. To operate a photomultiplier tube with good

Figure 20 : Effect of Dark Storage in Noise Reduction

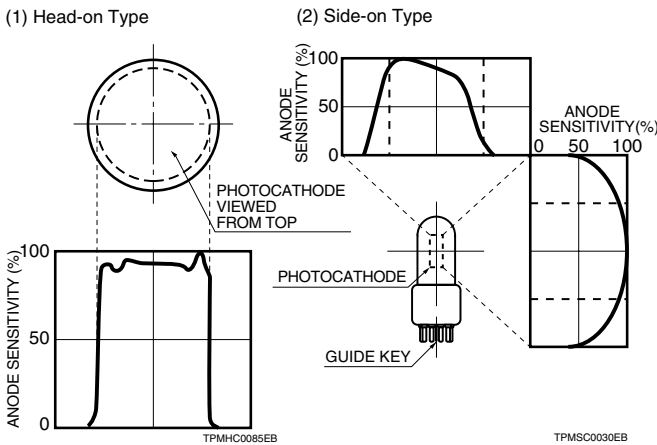


stability, it is necessary to leave the photomultiplier tube in dark state without allowing the incident light to enter the photocathode for about one or more hours. (This is called "dark storage" or "dark adaptation".) As Figure 20 shows, dark storage is effective in reducing the dark count rapidly in the actual measurement.

3-7 Uniformity

Uniformity is the variation in photomultiplier tube output with respect to the photocathode position at which light enters. As stated in 3-2 "Collection efficiency (CE)", even if uniform light enters the entire photocathode of a photomultiplier tube, some electrons emitted from a certain position of the photocathode are not efficiently collected by the first dynode (Dy1). This phenomenon causes variations in uniformity as shown in Figure 21. If photons enter a position of poor uniformity, not all the photoelectrons emitted from there are detected, thus lowering the detection efficiency. In general, head-on photomultiplier tubes provide better spatial uniformity than side-on photomultiplier tubes. For either type, good uniformity is obtained when light enters around the center of a photocathode.

Figure 21 : Typical Uniformity



3-8 Signal-to-Noise Ratio

This section describes theoretical analysis of the signal-to-noise consideration in both photon counting and analog modes. The noise being discussed here is mainly shot noise superimposed on the signal.

(1) Analog Mode

When signal light enters the photocathode of a photomultiplier tube, photoelectrons are emitted. This process occurs accompanied by statistical fluctuations. The photocathode signal current or average photocurrent I_{ph} therefore includes an AC component which is equal to the shot noise i_{ph} expressed below.

$$i_{ph} = \sqrt{2e I_{ph} B}$$

where e is the electron charge and B is the frequency bandwidth of the measurement system.

The shot noise which is superimposed on the signal can be categorized by origin as follows :

a) Shot Noise Resulting from Signal Light

Since the secondary electron emission in a photomultiplier tube occurs with statistical probability, the resulting output also has statistical fluctuation. Thus the noise current at anode, i_{sa} , is given by

$$i_{sa} = \sqrt{2e I_{ph} F B} \cdot \mu$$

where μ is the gain of the photomultiplier tube, F is the noise figure of the photomultiplier tube. If we let the secondary electron emission ratio per dynode stage be δ_n , the noise figure for the photomultiplier tube having n dynode stages can be expressed as follows:

$$F = \left(1 + \frac{1}{\delta_1} + \frac{1}{\delta_1 \cdot \delta_2} + \dots + \frac{1}{\delta_1 \dots \delta_n} \right)$$

Supposing that $\delta_1=5, \delta_2= \delta_3= \dots = \delta_n=3$, the noise figure takes a value of approximately 1.3 .

At this point, the photocurrent I_{ph} is given by

$$I_{ph} = \frac{P_i \eta(\lambda) \alpha e}{h \nu}$$

where P_i is the average light level entering the photomultiplier tube, $\eta(\lambda)$ is the photocathode QE at the wavelength λ , α is the photoelectron CE and $h\nu$ is the energy per photon.

b) Shot Noise Resulting from Background

As with the shot noise caused by signal light, the shot noise at the anode resulting from the background P_b can be expressed as follows:

$$i_{ba} = \sqrt{2e I_b F B} \cdot \mu$$

$$I_b = \frac{P_b \eta(\lambda) \alpha e}{h \nu}$$

where I_b is the equivalent average cathode current produced by the background light.

c) Shot Noise Resulting from Dark Current

Dark current may be categorized by cause as follows:

- ① Thermionic emission from the photocathode and dynodes.
- ② Fluctuation by leakage current between electrodes.
- ③ Field emission current and ionization current from residual gases inside the tube.

Among these, a major cause of the dark current is thermionic emission from the photocathode.

Therefore the shot noise resulting from anode dark current i_{da} can be expressed as shown below:

$$i_{da} = \sqrt{2eI_dFB} \cdot \mu$$

where I_d is the equivalent average dark current from the photocathode.

d) Noise from Succeeding Amplifier

When an amplifier with noise figure F_a is connected to the photomultiplier tube load, the noise converted into the input of the amplifier is given by

$$i_{amp} = \sqrt{\frac{4F_a kTB}{R_{eq}}}$$

where R_{eq} is the equivalent resistance used to connect the photomultiplier tube with the amplifier, T is the absolute temperature and k is the Boltzmann constant.

e) Signal-to-Noise Ratio

Taking into account the background noise ($I_b + I_d$), the signal-to-noise ratio (S/N) of the photomultiplier tube output becomes

$$S/N = \frac{I_{ph}}{\sqrt{2eFB\{I_{ph}+2(I_b+I_d)\} + (4F_a kTB/R_{eq})/\mu^2}} \dots (1)$$

Among the above equations, the amplifier noise can be generally ignored because the gain μ of the photomultiplier tube is sufficiently large, so the signal-to-noise ratio can be expressed as follows:

$$S/N \approx \frac{I_{ph}}{\sqrt{2eFB\{I_{ph}+2(I_b+I_d)\}}} \dots (1)'$$

f) Noise Equivalent Power

In addition, the noise can also be expressed in terms of noise equivalent power (NEP). The NEP is the light power required to obtain a signal-to-noise ratio of 1, that is, the light level to produce a signal current equivalent to the noise current. The NEP indicates the lower limit of light detection and is usually expressed in watts. From equation (1)' above, the NEP at a given wavelength can be calculated by using $I_b = 0$ and $S/N=1$, as follows:

$$S/N = \frac{I_{pha}}{\sqrt{2eF(I_{pha}+2I_{da})\mu B}} = \frac{Sp \cdot Pi}{\sqrt{2eF(SpPi+2I_{da})\mu B}}$$

where I_{pha} is anode signal current,
 I_{da} is anode dark current,
 and $I_{pha} = I_{ph} \cdot \mu = Sp \cdot Pi$

Sp : anode radiant sensitivity, Pi : input power

Then calculate the variable Pi

$$SpPi = \sqrt{2eF(SpPi+2I_{da})\mu B}$$

$$(SpPi)^2 - 2eF(SpPi+2I_{da})\mu B = 0$$

Therefore, NEP is given by Pi as follows:

$$Pi = \frac{eF\mu B}{Sp} + \frac{\sqrt{(eF\mu B)^2 + 4eFI_{da}\mu B}}{Sp}$$

In a low bandwidth region up to several kHz, the NEP mainly depends on the shot noise caused by dark current (the latter component in the above equation). In a high bandwidth region, the noise component (the former component in the above equation) resulting from the cathode radiant sensitivity (Sp/μ in the equation) predominates the NEP.

The noise can also be defined as equivalent noise input (ENI). The ENI is basically the same parameter as the NEP, and is expressed in lumens (Sp is measured in units of amperes per lumen in this case) or watts.

(2) Photon Counting Mode

In the analog mode, all pulse height fluctuations occurring during the multiplication process appear on the output. However, the photon counting mode can reduce such fluctuations by setting a discrimination level on the output pulse height, allowing a significant improvement in the signal-to-noise ratio.

In the photon counting mode in which randomly generated photons are detected, the number of signal pulses counted for a certain period of time exhibits a temporal fluctuation that can be expressed as a Poisson distribution. If we let the average number of signal pulses be N , it includes fluctuation (mean deviation) which is expressed in the shot noise $n = \sqrt{N}$. The amplifier noise can be ignored in the photon counting mode by setting the photomultiplier tube gain at a sufficiently high level, so that the discrimination level can be easily set higher than amplifier noise level.

As with the analog mode, dark current may be grouped by cause as follows:

(a) Shot noise resulting from signal light

$$n_{ph} = \sqrt{N_{ph}}$$

(N_{ph} is the number of counts by signal light)

(b) Shot noise resulting from background light

$$n_b = \sqrt{N_b}$$

(N_b is the number of counts by background light)

(c) Shot noise resulting from dark counts

$$n_d = \sqrt{N_d}$$

(N_d is the number of dark counts)

In actual measurement, it is not possible to detect N_{ph} separately. Therefore, the total number of counts ($N_{ph} + N_b + N_d$) is first obtained and then the background and dark counts ($N_b + N_d$) are measured over the same period of time by

removing the input light. Then N_{ph} is calculated by subtracting (N_b+N_d) from $(N_{ph}+N_b+N_d)$. From this, each noise component can be regarded as an independent factor, so the total noise component can be analyzed as follows:

Here, substituting $n_{ph} = \sqrt{N_{ph}}$, $n_b = \sqrt{N_b}$ and $n_d = \sqrt{N_d}$

$$n_{tot} = \sqrt{N_{ph} + 2(N_b + N_d)}$$

Thus the signal-to-noise ratio (S/N) becomes

$$S/N = \frac{N_{ph}}{n_{tot}} = \frac{N_{ph}}{\sqrt{N_{ph} + 2(N_b + N_d)}} \dots\dots\dots (3)$$

The number of counts per second for N'_{ph} , N'_b and N'_d is easily obtained as shown below, respectively. t is the measurement time in seconds.

$$N'_{ph} = N_{ph}/t, N'_b = N_b/t, \text{ and } N'_d = N_d/t$$

Accordingly, the equation (3) can be expressed as follows:

$$S/N = \frac{N'_{ph} \sqrt{t}}{\sqrt{N'_{ph} + 2(N'_b + N'_d)}} \dots\dots\dots (3)'$$

This means that the signal-to-noise ratio can be improved as the measurement time is made longer.

By replacing the measurement time and the number of counts per second with the corresponding frequency and current, with $t=1/(2B)$ and $N'_x=Ix/e$ ($e= 1.6 \times 10^{-19}$ C) respectively, it becomes clear that equation (1)' is equivalent to equation (3)' except for the noise figure term.

In photon counting mode, if we define the detection limit as the light level where the signal-to-noise ratio equals to 1, the number of signal count per second N_{ph} at the detection limit can be approximated below, from equation (3)' under the condition that the measurement time is one second and the background light can be disregarded.

$$N_{ph} \approx \sqrt{2N'_d} \text{ s}^{-1} \dots\dots\dots (4)$$

At this point, if the dark count N'_d is more than several counts per second, the detection limit can be approximated with an error of less than around 30 %.

If we let the QE at a wavelength λ (nm) be $\eta(\lambda)$, the

incident light power P_0 at the detection limit can be approximated as follows:

$$P_0 \approx \frac{2.8 \times 10^{-16} \cdot \sqrt{N'_d}}{\lambda \cdot \eta(\lambda)} \text{ W} \dots\dots\dots (5)$$

For your reference, let us calculate the power (P) of a photon per second as follows:

$$P = \frac{hc}{\lambda} \approx \frac{2 \times 10^{-16}}{\lambda} \text{ W}$$

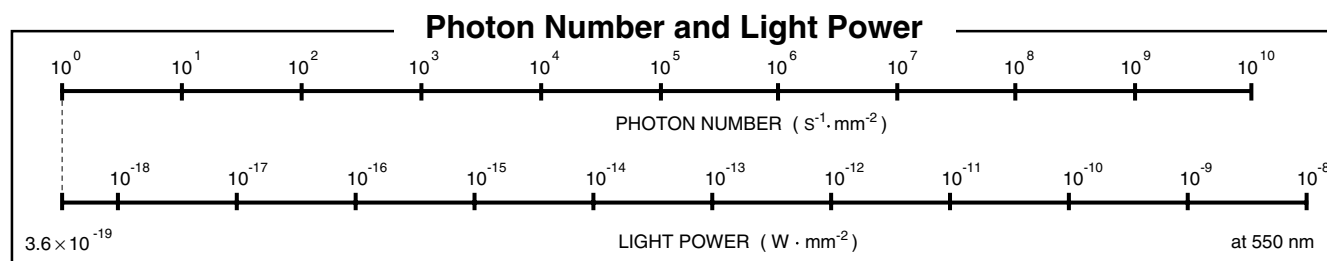
As an example, the illustration in the bottom of this page shows the relation between the light power and the number of photons at a wavelength of 550 nm.

In contrast to the signal pulse height distribution (PHD) similar to a Poisson distribution, the dark current pulses are distributed on the lower pulse height side. This is because the dark current includes thermal electrons not only from the photocathode but also from dynodes. Therefore, some dark current component can be effectively eliminated by setting a proper discrimination level without reducing much of the signal component. Furthermore, by placing an upper discrimination level, the photon counting mode can also eliminate the influence of environmental radiation which produces higher noise pulses and often cause significant problems in the analog mode. It is now obvious that the photon counting mode allows the measurement with a higher signal-to-noise ratio than in the analog mode, which is even greater contribution than that obtained from the noise figure F .

Reference

● Physical Constants

Constant	Symbol	Value	Unit
Electron Charge	e	1.602×10^{-19}	C
Speed of Light in Vacuum	c	2.998×10^8	m/s
Planck's Constant	h	6.626×10^{-34}	J·s
Boltzmann's Constant	k	1.381×10^{-23}	J/K
1 eV Energy	eV	1.602×10^{-19}	J
Wavelength in Vacuum Corresponding to 1 eV	—	1240	nm



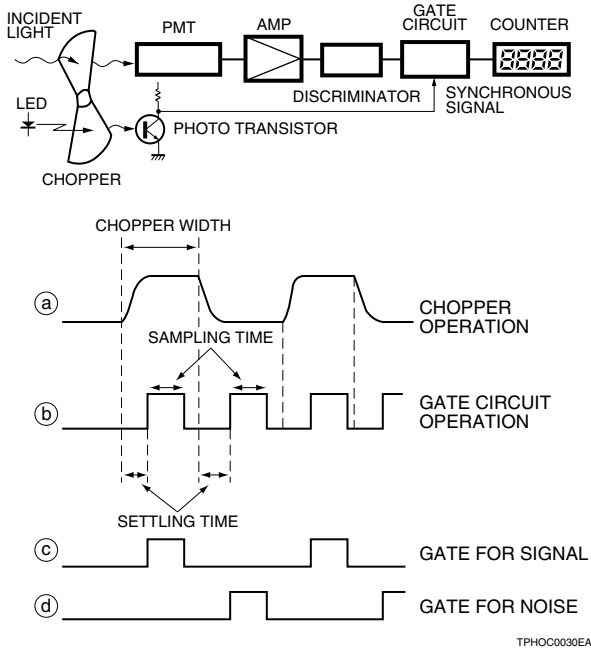
4. Measurement Systems

Photon counting can be performed with several measurement systems, including simple sequential measurements and sampling measurements depending on the information to obtain or the light level and signal timing conditions.

4-1 Synchronous Photon Counting Using Chopper

Using a mechanical chopper to interrupt incident light, this method makes light measurements in synchronization with the chopper operation. More specifically, signal pulses and noise pulses are both counted during the time that light enters a photomultiplier tube, while noise pulses are counted during light interruption for subtracting them from signal pulses and noise pulses. This method is effective when a number of noise pulses are present or when extremely low level light is measured. However, since this method uses a mechanical chopper, it is not suitable for the measurement of high-speed phenomena. This method is also known as the digital lock-in mode. Figure 22 shows a block diagram for this measurement system, along with the timing chart.

Figure 22 : Synchronous Photon Counting Using Chopper

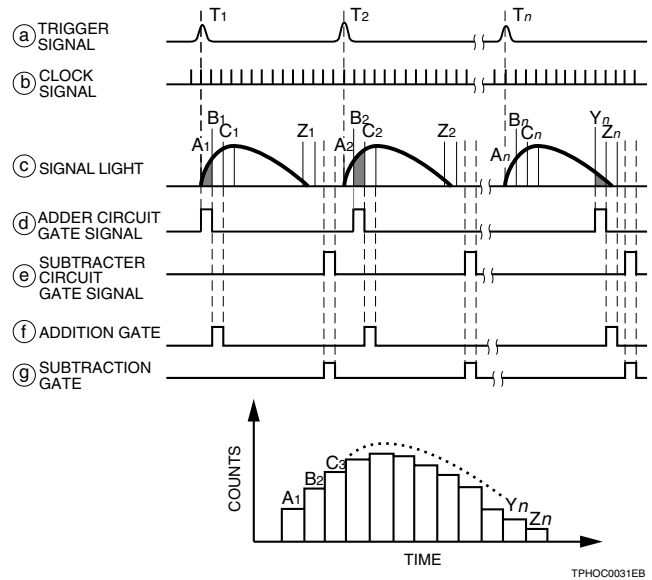


4-2 Time-Resolved Photon Counting by Repetitive Sampling

This method uses a pulsed light source to measure temporal changes of repetitive events. Each event is measured by sampling at a gate timing

slightly delayed from the repetitive trigger signals. The signal measured at each gate is accumulated to reproduce the signal waveform. This method is sometimes called the digital boxcar mode and is useful for the measurement of high-speed repetitive events. Figure 23 shows the time chart of this method.

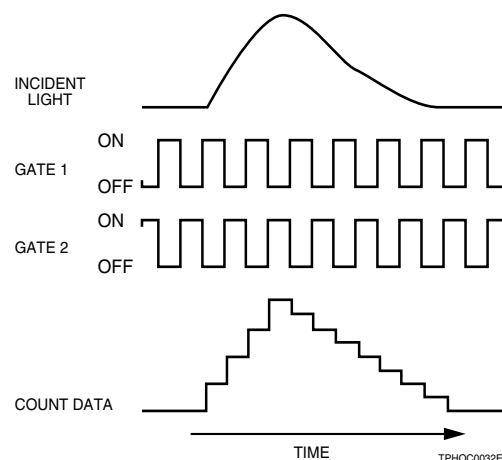
Figure 23 : Time-Resolved Photon Counting by Repetitive Sampling



4-3 Time-Resolved Photon Counting by Multiple Gates

This method sequentially opens multiple gates and measures the light level in a very short duration of the open gate, allowing a wide range of measurement from slow events to fast events. This method can also measure single events and random events by continuously storing data into memory. The time chart for this method is shown in Figure 24.

Figure 24 : Time-Resolved Photon Counting by Multiple Gates



4-4 Time-Correlated Photon Counting

Time-correlated photon counting (TCPC) is used in conjunction with a high-speed photomultiplier tube for fluorescence lifetime measurement (in tens of picoseconds to microseconds). By making the count rate sufficiently small relative to repetitive excitation light from a pulsed light source, this method measures time differences with respect to individual trigger pulses synchronized with excitation signals in the single photoelectron state.

Actual fluorescence and emission can be reproduced with good correlation by integrating the signals. Since this method only measures the time difference, it provides a better time resolution than the pulse width obtainable from a photomultiplier tube. A typical system for the TCPC consists of a high-speed preamplifier, a discriminator with less

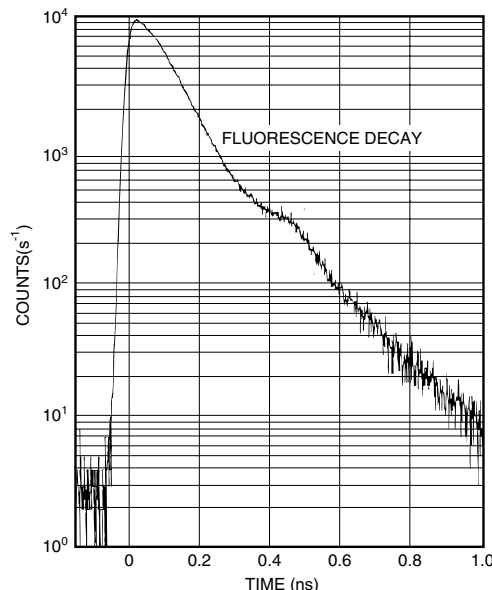
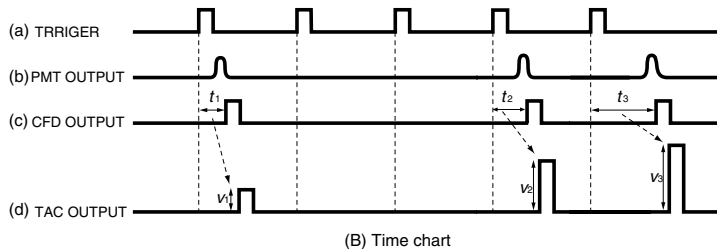
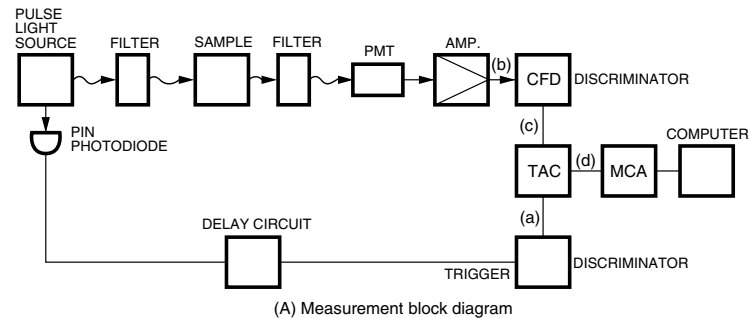
time jitter called a constant fraction discriminator (CFD), a time-to-amplitude converter (TAC), a multichannel pulse height analyzer (MCA) and a memory or computer. Figure 25 shows the block diagram, time chart for this measurement system and one example data for fluorescence decay time.

Besides TCPC, time-resolved measurement also includes phase difference detection using the modulation method. This method is sometimes selected due to advantages such as a compact light source and simpler operating circuits.

Reference: • "TECHNICAL INFORMATION Application of MCP-PMTs to time-correlated single photon counting and related procedures" (available from Hamamatsu).

• "TECHNICAL INFORMATION Modulated Photomultiplier Tube module H6573" (available from Hamamatsu)

Figure 25 : TCPC System



TFH0C0033ED

4-5 Calculating the Autocorrelation Function Using a Digital Correlator

Autocorrelation is a technique capable of finding repeated patterns in a signal or periodic signals in apparently irregular phenomena. Autocorrelation is a valuable technique for dynamic light scattering (DLS) and fluorescence correlation spectroscopy (FCS).

When measuring a signal output from a photodetector while viewing the signal intensity over time, and the signal intensities at a certain time t and another time delayed by τ are large, and this behavior repeatedly occurs, then that correlation is said to be high at time τ . The extent of this correlation can be expressed by the autocorrelation function.

When finding the autocorrelation function from the signal output by a photodetector, the autocorrelation function versus the time delay τ , $G(\tau)$, is expressed by equation (1). In the photon counting technique, $G(\tau)$ can also be calculated by equation (2) for time-series data containing the number of photons n_i detected per unit time (Δt : gate time) as the element. In each equation the values in $\langle \rangle$ are average values. M is the number of time-series data.

$$G(\tau) = \langle F(t)F(t+\tau) \rangle \quad \dots\dots\dots(1)$$

$$G(\tau) = G(k\Delta t) = \frac{1}{m} \sum_{i=1}^m n_i n_{i+k} \quad \because m = M - k \quad \dots\dots\dots(2)$$

Here, if the average of the signal intensity is $\langle F \rangle$, the signal intensities at times t and τ can be respectively expressed by using the fluctuations $\delta F(t)$ and $\delta F(t+\tau)$ as in $F(t) = \delta F(t) + \langle F \rangle$ and $F(t+\tau) = \delta F(t+\tau) + \langle F \rangle$. Equation (1) can therefore be rewritten as follows:

$$\begin{aligned} G(\tau) &= \langle (\delta F(t) + \langle F \rangle)(\delta F(t+\tau) + \langle F \rangle) \rangle \\ &= \langle \delta F(t)\delta F(t+\tau) \rangle + \langle F \rangle^2 \quad \dots\dots\dots(3) \\ &\because \langle \delta F(t) \rangle = \langle \delta F(t+\tau) \rangle = 0 \end{aligned}$$

From equation (3) we can see that the autocorrelation function is expressed by the intensity fluctuation term, $\langle \delta F(t)\delta F(t+\tau) \rangle$, and the square term of the average intensity, $\langle F \rangle^2$.

Here, the signal intensity fluctuation at time t , $\delta F(t)$, can be given by equation (4). If evaluating only the signal intensity fluctuation, the autocorrelation function can be obtained by calculating it by normalizing with the average signal intensity as in equation (5).

$$\delta F(t) = F(t) - \langle F \rangle \quad \dots\dots\dots(4)$$

$$\begin{aligned} g(\tau) &= \frac{\langle \delta F(t)\delta F(t+\tau) \rangle}{\langle F \rangle^2} \\ &= \frac{\langle (F(t) - \langle F \rangle)(F(t+\tau) - \langle F \rangle) \rangle}{\langle F \rangle^2} \\ &= \frac{\langle F(t)F(t+\tau) \rangle - \langle F \rangle^2}{\langle F \rangle^2} \quad \dots\dots\dots(5) \\ &\because \langle F(t) \rangle = \langle F(t+\tau) \rangle = \langle F \rangle \end{aligned}$$

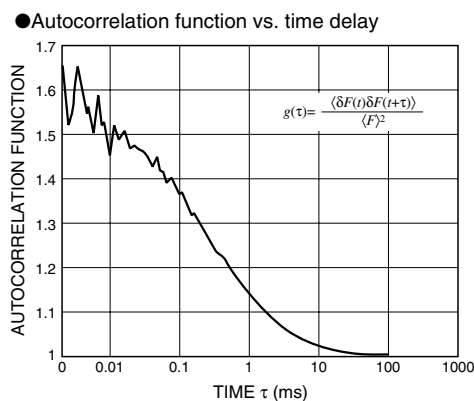
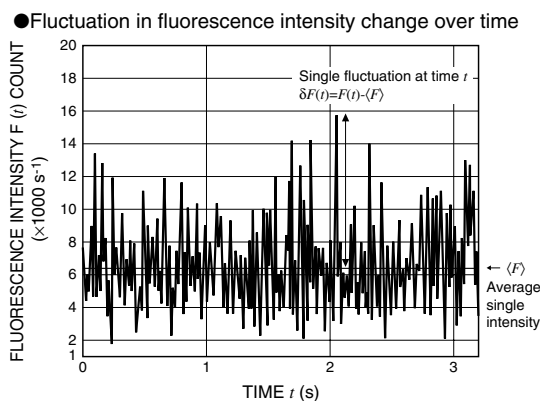
In the photon counting technique, equation (5) is converted to:

$$\begin{aligned} \langle F(t)F(t+\tau) \rangle &= \frac{1}{m} \sum_{i=1}^m n_i n_{i+k} \\ \langle F \rangle^2 &= \frac{1}{m^2} \sum_{i=1}^m n_i \sum_{i=1}^m n_{i+k} \end{aligned}$$

So the autocorrelation function can be obtained by equation (6) as follows:

$$g(k\Delta t) = \frac{m \sum_{i=1}^m n_i n_{i+k} - \sum_{i=1}^m n_i \sum_{i=1}^m n_{i+k}}{\sum_{i=1}^m n_i \sum_{i=1}^m n_{i+k}} \quad \dots\dots\dots(6)$$

Because calculating the autocorrelation function requires a great deal of time, the calculations were usually made by dedicated hardware correlators. However, recent improvements in computer processing speed now allow these calculations to be made by software. Our digital correlator (M9003+U8451) uses software to calculate the autocorrelation.



Fluctuation in fluorescence intensity change over time and its autocorrelation function

5. Selection Guide

This section describes how to select the optimum photomultiplier tube for photon counting, along with their brief specifications and related products. The following notes should be taken into account in selecting the photomultiplier tube that matches your needs.

5-1 Selecting The Photomultiplier Tube

(1) Photomultiplier Tube Structure

Photomultiplier tubes are roughly grouped into side-on and head-on types, so it is important to select the photomultiplier tube structure type according to the optical measurement conditions.

Side-on photomultiplier tubes have a rectangular photosensitive area and are therefore suitable for use in spectrophotometers where the output light is in the form of a slit, or for the detection of condensed light or collimated light.

Head-on photomultiplier tubes offer a wide choice of photosensitive areas from 5 mm to 120 mm in diameter and can be used under various optical conditions. Note, however, that selecting the photomultiplier tube with a photosensitive area larger than necessary may increase dark counts, thus deteriorating the signal-to-noise ratio.

(2) Photocathode Quantum Efficiency (QE)

The QE has direct effects on the detection efficiency. It is important to select a photomultiplier tube that provides high QE in the desired wavelength range.

(3) Gain

Gain required of the photomultiplier tube differs depending on the gain or equivalent noise input of the amplifier connected. As a general guide, it is advisable to select a photomultiplier tube having a gain higher than 1×10^6 , although it depends on the pulse width of the photomultiplier tube.

(4) Single Photoelectron Pulse Height Distribution (PHD)

Although not listed in the catalog, the PHD is an important factor since it relates to photomultiplier tube detection efficiency and stability. Hamamatsu designs photomultiplier tubes for photon counting, while taking the PHD into account. As a guide for estimating whether PHD is good or not, the peak to valley count ratio is sometimes used. (See Figure 6.)

(5) Dark Count → Lower Detection Limit

The dark count is an important factor for determining the lower detection limit of a photomultiplier tube. Selecting the photomultiplier tube with minimum dark counts is preferred. In general, for the same electrode structure, the dark count tends to increase with a larger photocathode and higher sensitivity in a long wavelength range. When a photomultiplier tube is used in a long wavelength range above 700 nm, cooling the photomultiplier tube is recommended.

(6) Response Time → Maximum Count Rate, Time Resolution

The maximum count rate (s^{-1}) in the photon counting mode is determined by the time response of the photomultiplier tube and the frequency characteristics of the signal processing circuit, or by the pulse width.

Most photomultiplier tubes have no problem with the time response up to a maximum count rate (random pulse) of $3 \times 10^6 s^{-1}$. However, in applications where the maximum count rate higher than this level is expected, a photomultiplier tube with the rise time (t_r) shorter than 5 ns must be selected. In time-correlated photon counting (TCPC), the electron transit time spread (TTS) is more important than the rise time itself.

5-2 Photomultiplier Tubes for Photon Counting

Table 6 (on pages 24 and 25) is a listing of typical Hamamatsu photomultiplier tubes designed or selected for photon counting, showing general specifications for the spectral response and configurations. For more information, refer to the Hamamatsu photomultiplier tubes catalog. In addition to the photomultiplier tubes listed in the table, you may choose from other Hamamatsu photomultiplier tubes for photon counting. Please consult our sales office.

5-3 Peripheral devices

There are many peripheral units and devices for photon counting. This section introduces photon counting units, photon counting heads, counting boards, high-voltage power supplies, coolers and amplifiers available from Hamamatsu, giving a brief description and specifications. For detailed information please refer to our product catalogs.

● Photon counting heads

Photon counting heads integrate a photomultiplier tube specially selected for photon counting, a high-voltage power supply and a photon counting circuit. Photon counting can be easily performed by simply counting the output signal pulses with a counting board or commercially available pulse counter. The supply voltage for the photomultiplier tube and the discrimination level are optimized so that no adjustments are required before use.

● PMT modules

- Photon counting type -

PMT modules include a photon counting photomultiplier tube and a high-voltage power supply. Using a PMT module with a photon counting unit or data acquisition unit allows you to easily perform photon counting.

● Counting boards, photon counting units

These devices are used to count the number of photoelectron pulses converted to logic (TTL) signals. Both PCI bus add-in board and USB interface types are provided. Our product lineup also includes high-speed types having a digital correlator function or capable of calculating the autocorrelation function. (See section 4-5.)

● Photon counting units

Photon counting units convert single photoelectron pulses detected by a photomultiplier tube or PMT module into a positive logic signal by using an internal photon counting circuit.

● Data acquisition units

Data acquisition units convert PMT module photoelectron pulses into a digital signal with a built-in photon counting circuit and send the count data to a PC.

● D-type socket assemblies

Hamamatsu provides a full line of D-type socket assemblies having a voltage divider circuit optimized for photon counting. Select a socket assembly that best matches the photomultiplier tube type to be used. D-type socket assemblies specifically designed for use with coolers are also provided.

The lineup also includes DP-type socket assemblies that incorporate a voltage divider circuit and a high-voltage power supply.

● High-voltage power supplies

The output from the photomultiplier tube fluctuates with changes in the supply voltage. To maintain stable photomultiplier tube operation, it is essential to select a high-voltage power supply that has minimal drift, ripple, and temperature dependence, as well as good input voltage and load regulation.

Hamamatsu high-voltage power supplies are designed to meet these requirements for high stability.

Power supplies come in various configurations including on-board types for mounting on PC boards, bench-top types for general use, and multi-output types for supplying high and low voltages.

● Coolers

Coolers are effective in reducing photomultiplier tube noise (dark count). We currently provide 4 cooler models each designed for use with various types of photomultiplier tubes.

● Amplifier units

Amplifier units are useful for compensating for photomultiplier tube gain. In photon counting, amplifier units should have a gain of at least 10 times (20 dB) and a frequency bandwidth of several dozen megahertz. Select an amplifier unit having the gain and frequency bandwidth that meet your application.

We also provide high-speed amplifier units that are ideal for fluorescence lifetime measurement.

● Power supply for PMT modules

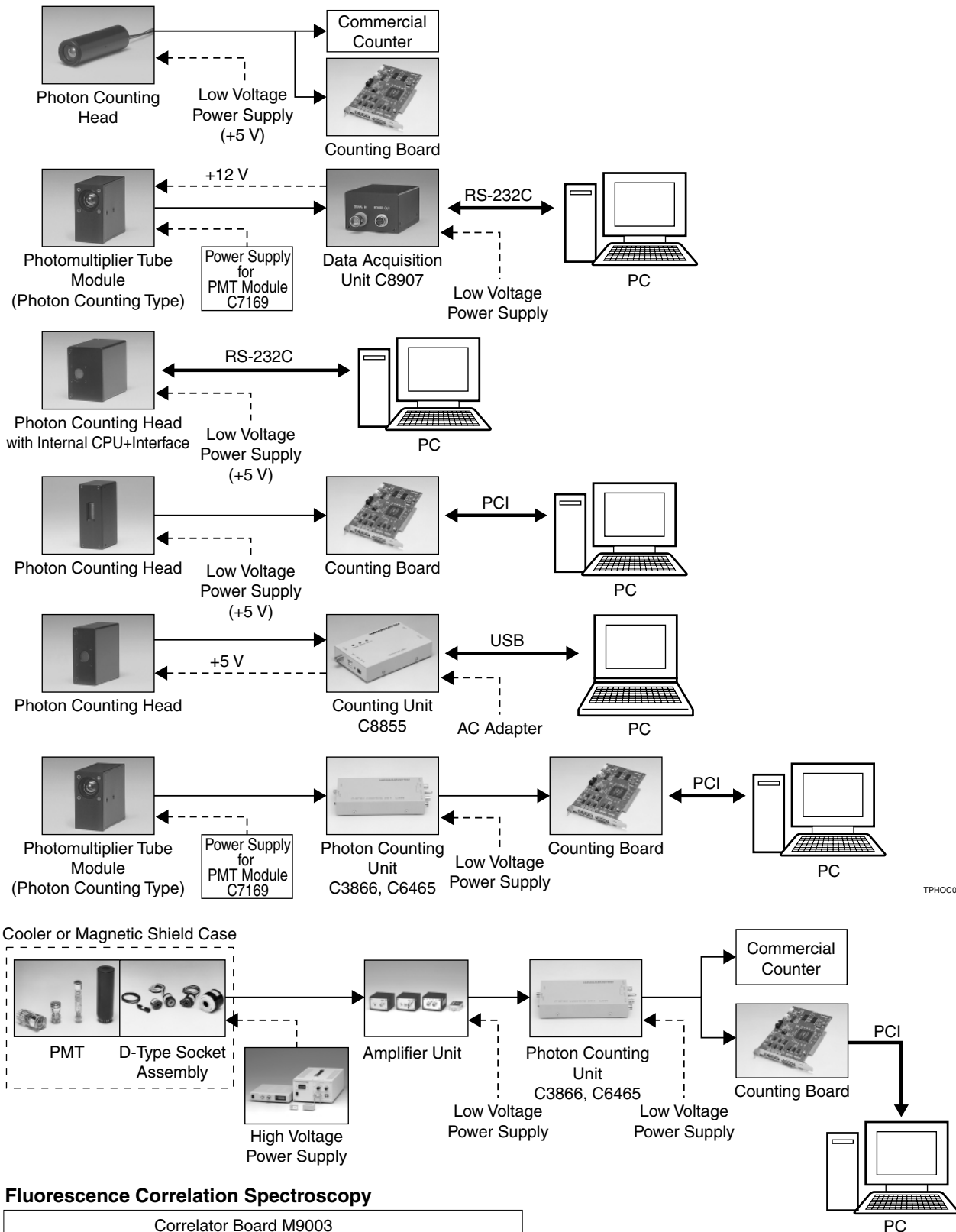
Integrated into a single unit, these power supplies provide the drive voltage (± 15 V) and control voltage (0 to 1.2 V) needed to operate a PMT module.

● Magnetic shield cases

Magnetic shield cases reduce adverse effects of magnetic fields all the way down to 1000th or even a 10 000th of their original strength to ensure photomultiplier tube stability. We have a complete lineup of magnetic shield cases for various sizes of photomultiplier tubes.

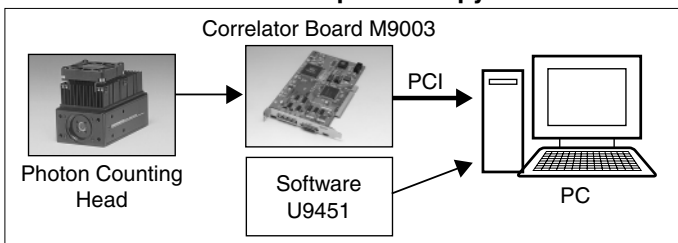
Related Products for Photon Counting

<Configuration Example>



TPHOC0047EA

Fluorescence Correlation Spectroscopy



TPHOC0161EA

Table 1: Photon Counting Head

Wavelength Region	Type No.	Spectral Response (nm)	Effective Area (mm)	Input Voltage DC (V)	Dark Count (s ⁻¹)		Count Linearity (s ⁻¹)	Note
					Typ.	Max.		
UV to Visible	H8259	185 to 680	4 × 20	+5	30	80	2.5 × 10 ⁶	
Visible	H7155	300 to 650	φ 8	+5	100	500	1.5 × 10 ⁶	
	H7155-20	300 to 650	φ 8	+5	100	500	1 × 10 ⁷	Internal prescaler of division by 4
	H7421-40	300 to 720	φ 5	+5	100	300	1.5 × 10 ⁶	High QE (40 % at 580 nm), cooled type
	H7828	300 to 650	φ 15	+5	200	500	1.5 × 10 ⁶	
	H7360-01	300 to 650	φ 22	+5	15	80	6.0 × 10 ⁶	Cable output
	H7360-02	300 to 650	φ 22	+5	60	300	6.0 × 10 ⁶	Cable output
	H7467	300 to 650	φ 8	+5	100	500	1.5 × 10 ⁶	Internal microprocessor and RS-232C interface
Visible to Near-Infrared	H9319	300 to 650	φ 22	+5	150	300	2 × 10 ⁷	Internal microprocessor, RS-232C interface and prescaler of division by 4
	H7421-50	380 to 890	φ 5	+5	125	375	1.5 × 10 ⁶	Cable output
	H7828-01	300 to 850	φ 15	+5	2000	3500	1.5 × 10 ⁶	
	H7360-03	300 to 850	φ 22	+5	5000	15 000	6.0 × 10 ⁶	Cable output
	H7467-01	300 to 850	φ 8	+5	600	1000	1.5 × 10 ⁶	Internal microprocessor and RS-232C interface
UV to Near-Infrared	H9319-02	300 to 850	φ 22	+5	10 000	15 000	2 × 10 ⁷	Internal microprocessor, RS-232C interface and prescaler of division by 4
	H8259-01	185 to 850	4 × 20	+5	80	200	2.5 × 10 ⁶	
	H8259-02	185 to 900	4 × 20	+5	400	800	2.5 × 10 ⁶	

Table 2: Photomultiplier Tube Module (Photon Counting Type)

Wavelength Region	Type No.	Spectral Response (nm)	Effective Area (mm)	Input Voltage DC (V)	Dark Count (s ⁻¹)		Rise Time (ns)	Note
					Typ.	Max.		
UV to Visible	H7732P-01	185 to 680	4 × 20	+15	30	80	2.2	
Visible	H5773P	300 to 650	φ 8	+15	80	400	0.78	Pin output
	H5783P	300 to 650	φ 8	+15	80	400	0.78	Cable output
	H7422P-40	300 to 720	φ 5	+15	100	300	1.0	Cooled type
	H7826P	300 to 650	φ 15	+15	200	500	1.5	
Visible to Near-Infrared	H7422P-50	380 to 890	φ 5	+15	125	375	1.0	Cooled type
	H7826P-01	300 to 850	φ 15	+15	2000	3500	1.5	
UV to Near-Infrared	H7732P-11	185 to 850	4 × 20	+15	80	200	2.0	

Table 3: Counting Board (Sample Software Supplied)

Type No.	Signal Input Level	Internal Counter Gate Time	Counter Gate Model	Interface	Compatible OS	Supply Voltage
M8784	TTL Positive logic	10 μs to 10 s (100 ns or more)*	Internal / External	PCI (half size)	Windows 98/98SE/Me/2000	5 V/1 A (Supplied from PCI bus)
C8855	TTL Positive logic	50 μs to 10 s	Internal only	USB (Ver. 1.1)	Windows 98/98SE/Me/2000	5 V/0.5 A (Supplied from accessory AC adapter)
M9003	TTL Positive logic	50 ns to 12.8 μs	Reciprocal mode / Gate mode	PCI (half size)	Windows 2000/XP Pro	5 V/1 A (Supplied from PCI bus)

* Counter gate mode: external

Table 4: Counting Unit

Type No.	Input Impedance (Ω)	Discrimination Level (Converted into input) (mV)	Gain Required in PMT	Prescaler	Maximum Count Rate (s ⁻¹)	Pulse Pair Resolution (ns)	Output Pulse	Output Pulse Width (ns)	Supply Voltage
C3866	50	-0.5 to -16	3 × 10 ⁶	1/1	4 × 10 ⁶	25	C-MOS	10	+5.2 ± 0.2 V, 150 mA/ -5.2 ± 0.2 V, 300 mA
				1/10	1 × 10 ⁷	10			
C6465	50	-2.2 to -31	5 × 10 ⁶	—	1 × 10 ⁶	60	TTL Positive Logic	30	+5 V, 60 mA/ -5 V, 120 mA

Table 5: Amplifier Unit

Type No.	Frequency Bandwidth (-3 db)	Voltage Gain (db)	Current-to-voltage Conversion Factor	Amplifier Input (Output)	Input Impedance (Ω)	Max. Output Signal Voltage (V)	Input Voltage (V)	Input Current (Max.) (mA)
C6438	DC to 50 MHz	20 ± 3 [Ⓐ] (approx. ×10)	0.5 mV/μA [Ⓑ]	±Voltage (non-inverted)	50	±1 [Ⓐ]	±5	±55
C9663	DC to 150 MHz	38 ± 3 [Ⓐ] (approx. ×80)	4 mV/μA [Ⓑ]	±Voltage (non-inverted)	50	±1.4 [Ⓐ]	±5	±80
C5594-44 [Ⓒ]	50 kHz to 1.5 GHz	36 ± 3 [Ⓐ] (approx. ×63)	3.15 mV/μA [Ⓑ]	±Voltage (non-inverted)	50	-2.5 [Ⓐ]	+12 to +16	+95

[Ⓐ]At 50 Ω load resistance.

[Ⓑ]Value after current-to-voltage conversion by input impedance.

[Ⓒ]Contact our sales office for other connectors for C5594.

MEMO

A series of horizontal dashed lines for writing.

Table 6: Typical Photomultiplier Tubes for Photon Counting

Wavelength Region	Configuration	Type No.	Spectral Response (nm)	Effective Area (mm)	Photocathode QE		Maximum Supply Voltage (V)
					QE Peak (%)	Wavelength (nm)	
VUV to UV	28mm side-on	R7154P	160 to 320	8 × 24	35	220	1250
UV to Visible	28mm head-on	R7207-01	160 to 650	φ 10	22	420	1500
	52mm head-on	R585	160 to 650	5 × 8	22	390	1500
	52mm head-on	R3235-01	160 to 650	φ 10	22	390	2500
	MCP-PMT	R3809U-52	160 to 680	φ 11	18	420	3400
	13mm side-on	R6350P	185 to 650	4 × 13	20	270	1250
	13mm side-on	R6353P	185 to 680	4 × 13	23	330	1250
	28mm side-on	R1527P	185 to 680	8 × 24	19	300	1250
	28mm side-on	R4220P	185 to 710	8 × 24	23	320	1250
	28mm side-on	R5983P	185 to 710	10 × 24	23	320	1250
Visible	28mm side-on	R7518P	185 to 730	8 × 24	30	300	1250
	10mm head-on	R1635P	300 to 650	φ 8	26	390	1500
	13mm head-on	R647P	300 to 650	φ 10	26	390	1250
	13mm head-on	R2557P	300 to 650	φ 10	20	375	1500
	16mm head-on	R7400P	300 to 650	φ 8	21	390	1000
	19mm head-on	R2295	300 to 650	φ 4	22	390	1250
	19mm head-on	R5610P	300 to 650	φ 15	20	375	1250
	25mm head-on	R1924P	300 to 650	φ 21	26	390	1250
	25mm head-on	R3550P	300 to 650	φ 21	20	375	1250
	28mm head-on	R7205-01	300 to 650	φ 10	22	420	1500
	28mm head-on	R6095P	300 to 650	φ 25	28	390	1000
	52mm head-on	R464	300 to 650	5 × 8	22	390	1500
	52mm head-on	R329P	300 to 650	φ 46	26	390	2700
	52mm head-on	R3234-01	300 to 650	φ 10	22	390	2500
Visible to Near-Infrared	19mm head-on	R1878	300 to 850	φ 4	20 0.3	340 800	1250
	28mm head-on	R7206-01	300 to 850	φ 10	20 0.4	420 800	1500
	28mm head-on	R2228P	300 to 900	φ 25	6 1	600 800	1500
	52mm head-on	R649	300 to 850	5 × 8	20 0.3	340 800	1500
	52mm head-on	R2257P	300 to 900	φ 46	8 0.2	600 800	2500
	52mm head-on	R3310-02	300 to 1010	10 × 10	13 0.25	340 1000	2200
UV to Near-Infrared	13mm head-on	R1463P	185 to 850	φ 10	22 0.3	270 800	1250
	28mm head-on	R1104P	185 to 850	φ 25	23 0.3	270 800	1500
	52mm head-on	R943-02	160 to 930	10 × 10	22 12	300 800	2200
	MCP-PMT	R3809U-50	160 to 850	φ 11	18 7	420 600	3400
	13mm side-on	R6358P	185 to 830	4 × 13	24 13	240 600	1250
	28mm side-on	R4632	185 to 850	8 × 24	26 11	270 600	1250
	28mm side-on	R928P	185 to 900	8 × 24	25 2.7	260 800	1250
	28mm side-on	R2949	185 to 900	8 × 6	25 2.7	260 800	1250
	28mm side-on	R636P	185 to 930	3 × 12	24 8	330 800	1500
	28mm side-on	R2658P	185 to 1010	3 × 12	14 0.13	330 1000	1500

Ⓐ Characteristics are measured at a supply voltage giving a gain of 2×10^5 .

Ⓑ Characteristics are measured at 1500 V regardless of gain.

Supply Voltage Typ. (V) (at 1×10^6 gain)	Dark Counts			Rise Time (ns)	TTS (ns)	Remarks	Type No.
	Typ. (s^{-1})	Max. (s^{-1})	Temp. ($^{\circ}C$)				
700	5	20	25	2.2	1.2		R7154P
770	10	30	25	1.7	1.2	Low Dark Counts, Low Afterpulse	R7207-01
800	5	15	25	13.0	—	Low Dark Count Type (Max. $3 s^{-1}$) available	R585
1500	50	150	25	1.3	0.45	Fast Time Response	R3235-01
3000 ^A	—	50	25	0.15	0.025	Fast Time Response	R3809U-52
750	10	30	25	1.4	0.75	Compact, Low Dark Counts	R6350P
800	5	10	25	1.4	0.75	Compact, High Sensitivity, Low Dark Counts	R6353P
780	10	50	25	2.2	1.2	Low Dark Counts	R1527P
730	10	50	25	2.2	1.2	High Sensitivity, Low Dark Counts	R4220P
720	10	50	25	2.2	1.2	Wide Photocathode Area	R5983P
730	10	50	25	2.2	1.2	High Sensitivity, Low Dark Counts	R7518P
1200	100	400	25	0.8	0.7	Compact	R1635P
900	80	400	25	2.5	1.6	Compact	R647P
1000	10	30	25	2.2	—	Low Noise Bialkali Photocathode	R2557P
900	80	400	25	0.78	0.23	Metal Package, Compact, Low Profile	R7400P
900	2	5	25	2.5	1.0	Low Afterpulse	R2295
850	15	45	25	1.5	—	Compact, Ruggedized	R5610P
1000	100	300	25	2.0	—	Ruggedized, Low Profile	R1924P
800	20	60	25	2.0	—	Low Profile, Low Dark Counts	R3550P
770	10	30	25	1.7	1.2	Low Dark Counts, Low Afterpulse	R7205-01
900	100	250	25	4.0	—		R6095P
1000	5	15	25	13.0	—	R464S (Max. $3 s^{-1}$) available	R464
1500	200	600	25	2.6	1.0		R329P
1500	50	150	25	1.3	0.45	Fast Time Response, Low Afterpulse	R3234-01
1100	100	250	25	2.5	1.0	Low Dark Counts, Low Afterpulse	R1878
770	300	1000	25	1.7	1.2	Low Dark Counts, Low Afterpulse	R7206-01
1100	150	500	-20	15.0	—	Extended-Red Multialkali Photocathode	R2228P
800	200	350	25	13.0	—	R649S (Max. $100 s^{-1}$) available	R649
1700	600	2000	-20	2.6	1.0	Extended-Red Multialkali Photocathode	R2257P
1700	30	150	-20	3.0	—	High Quantum Efficiency (at $1 \mu m$), For Raman Spectroscopy	R3310-02
1000	900	1000	25	2.5	—	Compact	R1463P
750	4500	7000	25	15.0	—	High Gain	R1104P
1700	20	50	-20	3.0	—	High Sensitivity	R943-02
3000 ^A	—	2000	25	0.15	0.025	Fast Time Response	R3809U-50
830	20	50	25	1.4	0.75	Compact, Low Dark Counts	R6358P
830	50	100	25	2.2	1.2	Low Dark Counts	R4632
720	500	1000	25	2.2	1.2	High Sensitivity	R928P
720	300 3	500 —	25 -20	2.2	1.2	Low dark counts	R2949
1300	15	50	-20	2.0	1.2	High Sensitivity	R636P
1500 ^B	50	300	-20	2.0	1.2	For UV to NIR range	R2658P

HAMAMATSU

HAMAMATSU PHOTONICS K.K., Electron Tube Division

314-5, Shimokanzo, Iwata City, Shizuoka Pref., 438-0193, Japan

Telephone: (81)539/62-5248, Fax: (81)539/62-2205

WEB SITE www.hamamatsu.com

Main Products

Electron Tubes

Photomultiplier Tubes
Light Sources
Microfocus X-ray Sources
Image Intensifiers
X-ray Image Intensifiers
Microchannel Plates
Fiber Optic Plates

Opto-semiconductors

Si Photodiodes
Photo IC
PSD
InGaAs PIN Photodiodes
Compound Semiconductor Photosensors
Image Sensors
Light Emitting Diodes
Application Products and Modules
Optical Communication Devices
High Energy Particle/X-ray Detectors

Imaging and Processing Systems

Video Cameras for Measurement
Image Processing Systems
Streak Cameras
Optical Measurement Systems
Imaging and Analysis Systems

Information in this catalog is believed to be reliable. However, no responsibility is assumed for possible inaccuracies or omission. Specifications are subject to change without notice. No patent rights are granted to any of the circuits described herein.

© 2005 Hamamatsu Photonics K.K.

Sales Offices

ASIA:

HAMAMATSU PHOTONICS K.K.
325-6, Sunayama-cho,
Hamamatsu City, 430-8587, Japan
Telephone: (81)53-452-2141, Fax: (81)53-456-7889

U.S.A.:

HAMAMATSU CORPORATION
Main Office
360 Foothill Road, P.O. BOX 6910,
Bridgewater, N.J. 08807-0910, U.S.A.
Telephone: (1)908-231-0960, Fax: (1)908-231-1218
E-mail: usa@hamamatsu.com

Western U.S.A. Office:

Suite 110, 2875 Moorpark Avenue
San Jose, CA 95128, U.S.A.
Telephone: (1)408-261-2022, Fax: (1)408-261-2522
E-mail: usa@hamamatsu.com

United Kingdom:

HAMAMATSU PHOTONICS UK LIMITED
Main Office
2 Howard Court, 10 Tewin Road Welwyn Garden City
Hertfordshire AL7 1BW, United Kingdom
Telephone: 44-(0)1707-294888, Fax: 44-(0)1707-325777
E-mail: info@hamamatsu.co.uk

South Africa Office:

PO Box 1112, Buccleuch 2066,
Johannesburg, South Africa
Telephone/Fax: (27)11-802-5505

France, Portugal, Belgium, Switzerland, Spain:

HAMAMATSU PHOTONICS FRANCE S.A.R.L.
8, Rue du Saule Trapu, Parc du Moulin de Massy,
91882 Massy Cedex, France
Telephone: (33)1 69 53 71 00
Fax: (33)1 69 53 71 10
E-mail: infos@hamamatsu.fr

Swiss Office:

Richtersmattweg 6a
CH-3054 Schüpfen, Switzerland
Telephone: (41)31/879 70 70,
Fax: (41)31/879 18 74
E-mail: swiss@hamamatsu.ch

Belgian Office:

7, Rue du Bosquet
B-1348 Louvain-La-Neuve, Belgium
Telephone: (32)10 45 63 34
Fax: (32)10 45 63 67
E-mail: epirson@hamamatsu.com

Spanish Office:

Centro de Empresas de Nuevas Tecnologías
Parque Tecnológico del Valles
08290 CERDANYOLA, (Barcelona) Spain
Telephone: (34)93 582 44 30
Fax: (34)93 582 44 31
E-mail: spain@hamamatsu.com

Germany, Denmark, Netherland, Poland:

HAMAMATSU PHOTONICS DEUTSCHLAND GmbH
Arzbergerstr. 10,
D-82211 Herrsching am Ammersee, Germany
Telephone: (49)8152-375-0, Fax: (49)8152-2658
E-mail: info@hamamatsu.de

Danish Office:

Skovbrynet 3, DK-5610 Assens, Denmark
Telephone: (45)4346/6333, Fax: (45)4346/6350
E-mail: lkoldbaek@hamamatsu.de

Netherlands Office:

PO Box 50.075, 1305 AB Almere The Netherland
Telephone: (31)36-5382123, Fax: (31)36-5382124
E-mail: info@hamamatsu.nl

Poland Office:

02-525 Warsaw, 8 St. A. Boboli Str., Poland
Telephone: (48)22-660-8340, Fax: (48)22-660-8352
E-mail: jbaszak@hamamatsu.de

North Europe and CIS:

HAMAMATSU PHOTONICS NORDEN AB
Smidesvägen 12
SE-171 41 Solna, Sweden
Telephone: (46)8-509-031-00, Fax: (46)8-509-031-01
E-mail: info@hamamatsu.se

Russian Office:

Riverside Towers
Kosmodamianskaya nab. 52/1, 14th floor
RU-113054 Moscow, Russia
Telephone/Fax: (7)095 411 51 54
E-mail: info@hamamatsu.ru

Italy:

HAMAMATSU PHOTONICS ITALIA S.R.L.
Strada della Moia, 1/E
20020 Arese, (Milano), Italy
Telephone: (39)02-935 81 733, Fax: (39)02-935 81 741
E-mail: info@hamamatsu.it

Rome Office:

Viale Cesare Pavese, 435, 00144 Roma, Italy
Telephone: (39)06-50513454, Fax: (39)06-50513460
E-mail: inforoma@hamamatsu.it